Journal of Power Sources 454 (2020) 227932

Contents lists available at ScienceDirect

Journal of Power Sources

journal homepage: www.elsevier.com/locate/jpowsour

Progress and challenges of flexible lithium ion batteries

Zhenhan Fang [a,b,1], Jing Wang [a,b,1], Hengcai Wu [a,b], Qunqing Li [a,b,c], Shoushan Fan [a,b], Jiaping Wang [a,b,c,*]

[a] Department of Physics, Tsinghua University, Beijing, 100084, PR China
[b] Tsinghua-Foxconn Nanotechnology Research Center, Tsinghua University, Beijing, 100084, PR China
[c] Frontier Science Center for Quantum Information, Beijing, 100084, China

HIGHLIGHTS

- The latest progress of flexible lithium batteries (FLIBs) is reviewed.
- Two research routes to achieve FLIBs are summarized.
- The challenges of FLIBs in material selection and structural design are analyzed.
- The key points of future development of FLIBs are listed.

ARTICLE INFO

Keywords:
Lithium ion batteries
Flexible
Energy density

ABSTRACT

The research in high performance flexible lithium ion batteries (FLIBs) thrives with the increasing demand in novel flexible electronics such as wearable devices and implantable medical kits. FLIBs share the same working mechanism with traditional LIBs. Meanwhile, FLIBs need to exhibit flexibility and even bendable and stretchable features. The development of FLIBs highly relies on the improvement of flexible electrodes and battery designs to achieve high performance and stability under mechanical deformation. In this review, recent advances and progress on the development of FLIBs are concerned. Two specific research strategies of FLIBs are discussed in detail: preparation of flexible battery components (including electrodes, current collectors, and electrolytes) and flexible structure designs or assembly methods of FLIBs. Finally, challenges and perspectives for developing high performance FLIBs are presented.

1. Introduction

With the gradual miniaturization, high-speed, and high integration of portable electronics, flexible electronic devices have emerged and are widely used in communications [1], healthcare [2,3], and wearable consumer electronics [4–6]. As the energy sources in these flexible electronic devices, high-performance flexible batteries play an indispensable role. Flexible batteries incorporate all the functional attributes of conventional batteries in formats that have been altered to withstand mechanical deformations such as bending, stretching, distorting, and folding. Compared with traditional batteries, flexible batteries have great advantage in resistance to mechanical deformation, which enable electronic products perform well in a variety of conditions. More application scenarios are envisioned with the development of flexible batteries. For example, flexible batteries can replace traditional batteries as power supply components in implantable medical devices. The characteristics of flexible batteries make it easier to match the medical devices with the requirements of human body structures [7].

In 1980, Goodenough et al. found that layered lithium cobalt oxide ($LiCoO_2$) material allowed reversible intercalation and deintercalation of lithium ions at a high potential, which became a milestone in the history of LIB development [8]. Subsequently, researchers found that lithium ions can be repeatedly inserted and removed from graphite structure at a low potential. With lithium cobaltate as the cathode and graphite as the anode, reversible charging and discharging processes can be achieved in LIBs through repeated migration of lithium ions between the cathode and the anode [9]. Based on this mechanism, Sony first realized the commercialization of LIBs in 1991. Since then, LIBs have

* Corresponding author. Department of Physics, Tsinghua University, Beijing, 100084, PR China.
E-mail address: jpwang@tsinghua.edu.cn (J. Wang).
[1] These authors contributed equally to this work.

https://doi.org/10.1016/j.jpowsour.2020.227932
Received 23 January 2020; Received in revised form 18 February 2020; Accepted 19 February 2020
Available online 25 February 2020
0378-7753/

been extensively explored by many researchers for more than 20 years. The 2019 Nobel Prize in chemistry has been awarded to Professors J. B. Goodenough, M. S. Whittingham, and A. Yoshino for their great contributions to the development of LIBs. Until now, LIBs have been the most widely used energy storage system in electric vehicles and portable electronic devices, and are a suitable choice for use as FLIBs due to the advantages of light weight, high energy density, large specific energy, small self-discharge, no memory effect, stable cycle performance, fast charge-discharge, and environmental friendliness [10].

FLIBs have the same working mechanism with traditional LIBs, but need to maintain their electrochemical performances under repeated mechanical deformation in actual operation. At present, the existing LIBs materials themselves are not flexible, and FLIBs faces the following challenges: (i) how to adapt the battery material to the flexible application scenario? (ii) how to maintain good contact between active material particles and other components (conductive agent, current collector, and electrolyte) and reduce the contact resistance? (iii) how to avoid the leakage of the electrolyte? (iv) how to increase the active material loading and achieve both high energy density and great flexibility?

In this review, the most recent literature on FLIBs are collected and summarized. For traditional LIBs, research mainly focuses on the investigation of new electrode materials, while research for FLIBs concentrates on the flexible characteristics of batteries. As shown in Fig. 1, there are mainly two specific research strategies of FLIBs: one is to make flexible battery components such as electrode, current collector, and electrolyte; the other is to maintain excellent electrochemical properties of FLIBs under mechanical deformation by flexible structural designs or novel assembly methods. The characteristics, advantages, and challenges of these two strategies will be discussed in detail in this review.

2. Flexible battery components

FLIBs are required to maintain excellent mechanical and electrochemical properties under repeated mechanical deformation. One of the most feasible ways to obtain FLIBs is to make all the battery components, especially electrodes and electrolytes, flexible.

2.1. Flexible electrodes

The development of flexible electrodes is the key to achieve high-performance FLIBs. In general, electrodes are prepared by coating slurry on conductive metal substrates. However, electrode materials tend to detach from the rigid metal current collectors during mechanical deformation, resulting in capacity loss and inferior electrochemical performance. In order to construct flexible electrodes, it is necessary to focus on both active materials and substrates. Recently, there have been the following common strategies to develop flexible electrodes: (i) Applying flexible carbon materials as conductive substrates to load active materials. (ii) Using flexible polymers as conductive materials or binders in the flexible electrodes. (iii) Constructing flexible electrodes based on MXene materials. In this section, the assembly and preparation methods of flexible electrodes are reviewed. The relationship between the components in flexible electrodes and the electrochemical performance of batteries is analyzed. The challenges faced by flexible electrodes are also discussed.

2.1.1. Carbon materials

Current collector is a necessary component to support active materials and conduct electrons. The commonly used current collectors are metals such as aluminum (Al) and copper (Cu), which are heavy and often exhibit weak adhesion with electrode materials. Therefore, the use of metal current collectors in FLIBs causes the problems of capacity loss, low energy density, and poor rate performance during repeated mechanical deformation. Carbon materials, such as carbon nanotubes (CNTs), graphene, and carbon nanofibers (CNFs), exhibit excellent thermal and chemical stability, high electrical conductivity, and outstanding mechanical properties. Therefore, carbon materials are often used as self-supporting flexible electrodes in FLIBs to eliminate the need for metal current collectors [11–13].

CNTs are widely researched as conductive additive or current collector in LIBs. CNTs construct a conductive network that provide pathways for electrons in the electrodes. In addition, CNTs can be assembled to build a membrane that works as a flexible substrate. Free-standing CNT-based materials with light weight, great flexibility, chemical stability, and high conductivity are promising for producing flexible electrodes.

CNT film with excellent flexibility and low density can function as a promising type of current collectors for FLIBs with high energy density. Wang et al. fabricated flexible CNT current collectors by cross-stacking continuous CNT films drawn from super-aligned CNT (SACNT) arrays (Fig. 2a) [14]. Compared with the graphite/Cu interface, better wetting,

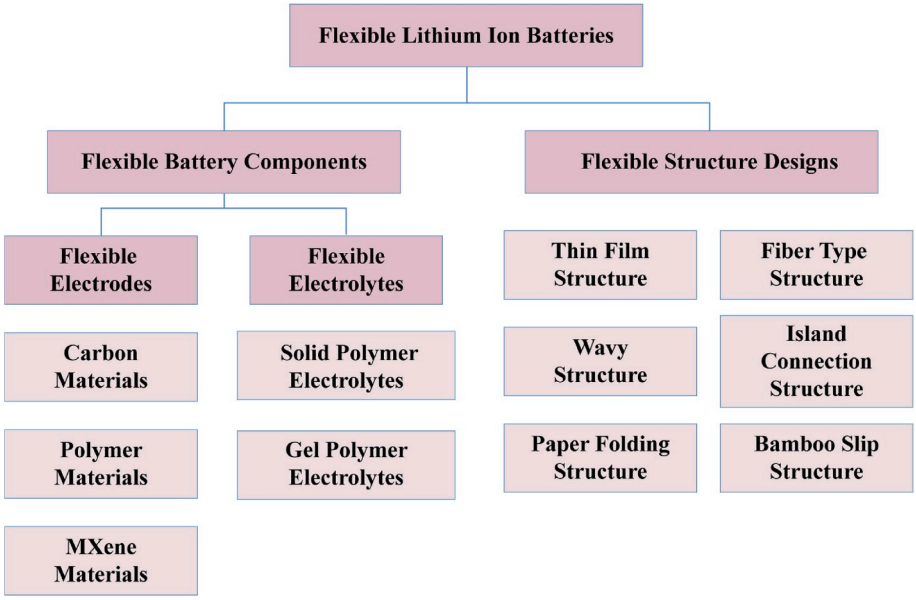

Fig. 1. Research strategies of FLIBs.

stronger adhesion, greater mechanical durability, and lower contact resistance were demonstrated at the graphite/CNT interface. The graphite-CNT anode showed excellent cycling stability and rate capability (335 mA h g^{-1} at 0.1 C and 326 mA h g^{-1} at 2 C), and more than 180% improvement in gravimetric energy density than the graphite/Cu anode due to the extremely low areal density of the CNT film (0.04 mg cm^{-2}). Wu et al. also fabricated CNT current collectors using horizontally oriented, ultralarge CNT macrofilms (HUCNMs) with low electrical resistance and good electrolyte wettability [15]. Batteries based on these CNT current collectors exhibited excellent stability upon folding, and these foldable LIBs can serve as power sources for wearable devices.

In addition to current collectors, both conductive additives and binders are commonly used in traditional electrodes. The conductive additives provide pathways for electrons and the binders connect components together. However, the introduction of these electrochemically inactive components reduces the energy density of the electrodes. As CNTs can construct a self-supporting framework, flexible electrodes with minimized amounts of conductive additives and binders can be obtained by the integration of the CNT framework with active materials. For example, binder-free $LiCoO_2$-CNT composite cathodes were fabricated by an ultra-sonication and co-deposition technique [16]. CNTs acted as both conductive additive and structural framework, and $LiCoO_2$ particles were uniformly embedded in the continuous CNTs network (Fig. 2b). The $LiCoO_2$-CNT electrodes showed high conductivity and great flexibility. Meanwhile, the porous structure of the cathodes facilitated electrolyte infiltration and accommodated volume change of the electrode. The $LiCoO_2$-CNT electrodes exhibited outstanding cycling stability and rate performance (151.4 mA h g^{-1} at 0.1 C with retention of 98.4% over 50 cycles and 137.4 mA h g^{-1} at 2 C). Furthermore, the binder-free $LiCoO_2$-CNT composites showed a 20.6% increase in specific mass capacity and 64% increase in specific volume capacity than the traditional $LiCoO_2$-Super P cathode with binder. As another example, an in-situ, scalable sol-gel method was used to prepare a TiO_2/CNT hybrid film as an anode in FLIBs [17]. The TiO_2/CNT anodes inherited the high flexibility of the CNT framework and demonstrated enhanced rate capability and charge/discharge reversibility with a pseudocapacitive storage mechanism. The anodes tested in half cells exhibited a discharge capacity of 100 mA h g^{-1} at 60 C over 1000 cycles, and a flexible full cell showed negligible capacity decay over 500 cycles of bending. Almheiri et al. fabricated flexible, foldable, and freestanding multiwalled CNT-Fe_2O_3 (MWCNT-Fe_2O_3) electrodes by a tape casting method and investigated the effect of the ratio of the active materials on the electrochemical performance [18]. The MWCNT-Fe_2O_3 electrodes with high Fe_2O_3 mass ratio showed high energy density and those with low Fe_2O_3 mass ratio exhibited high power density, demonstrating the potential of these electrodes for use in various applications. Dong et al. synthesized putty-like MnO_2/CNT nanostructured composites by mixing MnO_2 colloidal nanosheets with CNTs under vigorous mechanical stirring and worked as anodes for LIBs (Fig. 2c) [19]. The layered structure of MnO_2 afforded interlayered voids for fast and reversible lithium ions insertion/extraction. The flexible CNTs among the MnO_2 nanosheets acted as conductive additives, expanded the electron transport pathway, and made the whole structure stable and resistive to deformation during the charge/discharge processes. Moreover, with the addition of CNTs, the composites were flexible and could be molded into various shapes. The MnO_2/CNT electrodes displayed a high-specific capacity of 796 mA h g^{-1} at a current density of 500 mA g^{-1} and maintained a specific capacity of 236 mA h g^{-1} at a high current density of 10 A g^{-1}.

Graphene is another promising material in the field of electrochemical energy storage due to its large surface area, low weight, good

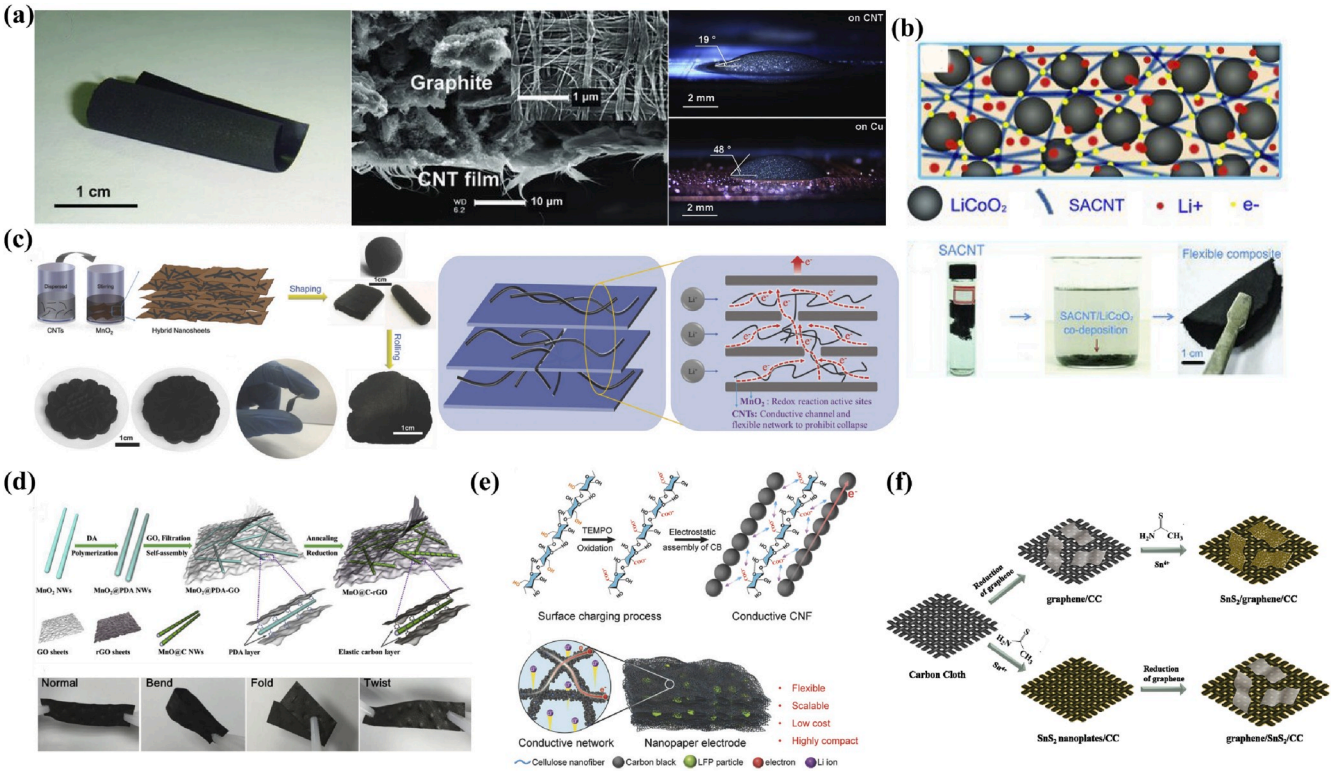

Fig. 2. (a) Photograph and cross-sectional SEM image of a flexible graphite electrode with a CNT current collector, and photographs of graphite slurry droplets on a CNT film and a Cu foil [14]. Reproduced with permission. Copyright 2013, Wiley-VCH. (b) Schematic of the structure and the preparation of a binder-free $LiCoO_2$-SACNT cathode [16]. Reproduced with permission. Copyright 2012, Wiley-VCH. (c) Schematic of synthesis and photographs of a flexible MnO_2-CNT composite [19]. Reproduced with permission. Copyright 2018, Wiley-VCH. (d) Schematic of the preparation process and photographs of a MnO@C-rGO electrode at different deformation status [21]. Reproduced with permission. Copyright 2019, Elsevier, Inc. (e) Schematic of the formation mechanism of conductive CNF and the hierarchical structure of the nanopaper electrode [29]. Reproduced with permission. Copyright 2018, Wiley-VCH. (f) Schematic of the synthesis of SnS_2-graphene-CC electrodes [32]. Reproduced with permission. Copyright 2019, Elsevier, Inc.

chemical and thermal stability, high electrical conductivity, and superior mechanical flexibility [20]. Graphene demonstrates the following better performances than CNTs: (i) The theoretical specific surface area of graphene is higher than that of CNTs, and the larger surface area provides more active sites for electrochemical reactions. (ii) It is easier to disperse graphene in solution than CNTs, so the preparation of graphene-based composites is more feasible.

Graphene-based composites are usually fabricated by deriving from graphene sheets. Ma et al. fabricated flexible electrodes through vacuum-assisted layer-by-layer assembly of one dimensional (1D) polydopamine coated MnO_2 nanowires (MnO_2@PDA NWs) and two dimensional (2D) graphene oxide nanosheet (GO NS) (Fig. 2d) [21]. The electrodes had a hierarchical void-containing structure with MnO_2 NWs encapsulated by a carbon layer and interconnected reduced GO sheets. The three dimensional (3D) robust structure provided continuous networks and pathways for electron and ion transport, and yielded abundant internal voids to accommodate any volume change during the charge/discharge processes. The composites delivered reversible capacities of 920 mA h g^{-1} at 0.2 A g^{-1} and 396 mA h g^{-1} at 10 A g^{-1}. The full cell showed high mechanical flexibility, a specific capacity of 2.6 mA h cm^{-2} at current density of 0.5 mA cm^{-2}, and a capacity retention of 90% after bending for 100 cycles. Zhang et al. fabricated free-standing SnS_2/graphene nanocomposite papers by vacuum filtration and two-phase hydrothermal processes [22]. The composites performed well due to the conductive and flexible graphene matrix, which accommodated the volumetric change of SnS_2 during electrochemical processes.

Graphene sheets have high inherent electrical conductivity. However, the high inter-sheet junction contact resistance has been a challenge in developing high performance graphene based electrodes. Many researchers have explored novel ways to solve this problem. Cheng et al. fabricated 3D graphene foams (GFs) by template-directed chemical vapor deposition [23]. The GFs showed high specific surface area and outstanding electrical and mechanical properties, and the GFs loaded with $Li_4Ti_5O_{12}$ and $LiFePO_4$ were used as the anode and the cathode in a thin, lightweight FLIB [24]. The 3D porous structure of $Li_4Ti_5O_{12}$/GF hybrid anode produced a highly conductive pathway for electron transfer, and provided a fast transport channel for lithium ion flux, suggesting its potential for fast charge and discharge. The $Li_4Ti_5O_{12}$/GF anodes were examined at a high rate up to 200 C and retained a specific capacity of 135 mA h g^{-1}. The $LiFePO_4$/GF-$Li_4Ti_5O_{12}$/GF full cell exhibited a specific capacity of 98 mA h g^{-1} at 50 C. Moreover, the high rate performance and long-life cyclic performance of the full cell can be maintained under repeated bending to a radius of 5 mm, suggesting the high flexibility of the electrode. Xu et al. designed a 3D graphene (3DG) aerogel and fabricated 3DG/metal-organic framework composites by an excessive metal-ion-induced combination and spatially confined Ostwald ripening strategy [25]. The composites were further transformed into 3DG/Fe_2O_3 aerogels with porous Fe_2O_3 frameworks well encapsulated within graphene sheets. The hierarchical structure of the aerogel offered a porous conductive network, abundant stress buffering nanospace for effective charge transport, intimate contact between graphene and porous Fe_2O_3, and robust structural stability during electrochemical processes. The free-standing 3DG/Fe_2O_3 aerogel was used as a flexible anode for FLIBs and showed an outstanding capacity of 1129 mA h g^{-1} at 0.2 A g^{-1} after 130 cycles and excellent cycling stability with a capacity retention of 98% after 1200 cycles at 5 A g^{-1}.

In order to further improve the chemical reactivity of graphene, nitrogen (N) doping has widely been introduced. Rooney et al. developed 3D graphene foams with encapsulated germanium (Ge) quantum dot/nitrogen-doped graphene yolk-shell nano architecture [26]. The yolk-shell structure alleviated the volume expansion/contraction during the electrochemical processes and enabled the formation of stable solid electrolyte interface (SEI) on the N-doped graphene outer shell, preventing electrolyte infiltration through the outer shell. The N-doped graphene outer shell minimized the pulverization, exfoliation, and aggregation of Ge. The 3D interconnected porous structure facilitated fast lithium ion and electron diffusion. The composite exhibited a high specific reversible capacity of 1220 mA h g^{-1}, long cycling capability of over 96% capacity retention, and high rate capability of over 800 mA h g^{-1} at 40 C.

CNF is a 1D inorganic polymer fiber with carbon content higher than 90%, has excellent electrochemical stability and robust mechanical property, and shows great potential in the fabrication of flexible and free-standing electrodes [27,28]. CNF can construct a conductive self-standing and flexible network. Hu et al. reported a conductive nanofiber network by a conformal electrostatic assembly of neutral carbon black particles on cellulose nanofibers (Fig. 2e) [29]. Due to the interconnected nanopores, the conductive nanofiber network provided both electron and ion transfer pathways, and enabled a high loading of $LiFePO_4$ particles (up to 60 mg cm^{-2}). The LIBs based on the conductive nanofiber network demonstrated area capacity of 8.8 mA h cm^{-2}, energy densities of 30 mWh cm^{-2} and 538 Wh L^{-1}, and excellent cycling stability with 91% capacity retention after 150 cycles. The pouch cell possessed good durability during repeated folding and bending tests. Active materials can also be wrapped in CNF. Yu et al. constructed 3D hierarchical Fe_2O_3@CNFs@MoS_2 fabric films as self-standing and robust anodes by electrospinning [30]. The Fe_2O_3 nanoparticles were encapsulated in the CNF skeleton, and the ultrathin curly MoS_2 nanosheets were tightly anchored onto the surface of the interconnected Fe_2O_3@CNF substrate. The flexible Fe_2O_3@CNFs skeleton established a 3D continuous conducting network and maintained structural integrity of the electrode. Meanwhile, the MoS_2 nanosheets shortened the length of lithium ion diffusion path, and offered more active sites for reversible lithium ion insertion/extraction reactions. A quasi-solid-state flexible full cell with the $LiCoO_2$ cathode, the poly(vinylidene fluoride)/poly (propylene carbonate) (PVDF/PPC) gel polymer electrolyte, and the Fe_2O_3@CNFs@MoS_2 fabric anode delivered an areal specific capacity of 6.47 mA h cm^{-2} and capacity retention of 90.8% after 300 cycles even in the 90° bending position. Huang et al. reported a water-steam selective etching strategy to create pores on CNF, and transition metal oxides were embedded into the fiber [31]. The mechanical stress from bending was released by the pores on CNF, and the composites effectively accommodated the volume change and enhanced the kinetics of ion and electron transport. A FLIB using the steam-etched Fe_2O_3@CNF anode and $LiFePO_4$/CNF cathode delivered a high capacity of 623 mA h g^{-1} at 100 mA g^{-1}, and stable electrochemical performances were achieved under the bent state.

Carbon cloth (CC) made by CNF was also widely used. Huang et al. developed a freestanding binder-free electrode with SnS_2 nanoflake arrays decorated on graphene supported by CC (Fig. 2f) [32]. The SnS_2/graphene/CC electrode possessed a 3D network architecture and a large specific surface area to enable high mass loading of active materials. The CC worked as a current collector and greatly enhanced the electrical conductivity of the electrodes. The composites were flexible and could be rolled up because of the excellent mechanical properties of the CC. The electrode delivered a large initial discharge capacity of 1987.4 mA h g^{-1} and capacity of 638.1 mA h g^{-1} after 150 cycles with coulombic efficiency of around 100%.

To summarize, high-performance flexible electrodes can be constructed based on carbon materials due to the following advantages: (i) Carbon materials build a robust and flexible network in the electrodes to accommodate repeated mechanical deformation. (ii) Carbon materials have high conductivity and the network is porous, so the network can provide pathways for both ion and electron transportation to enhance electrochemical kinetics. (iii) The porous network can buffer the volume change of the active materials during charge/discharge processes to maintain stable structures of the electrodes. (iv) Carbon materials have a large surface area and low interface resistance to provide abundant active sites for electrochemical reaction. (v) Carbon materials have good electrolyte wettability and strong adhesion to active materials, which enhance the cycle stability and rate capability of the electrodes. (vi) Carbon materials are lightweight compared to metal foil, which is

beneficial to increase the energy density of LIBs. However, there still exist some problems for the electrodes based on carbon materials. (i) These electrodes often suffer from irreversible capacity, low initial coulombic efficiency, and capacity fading because of the side reaction between carbon materials and electrolytes that arises from the functional groups and the defects of carbon materials. (ii) Both the loading of active materials and the conductivity of the electrodes should be considered, because high loading of insulating active materials on carbon materials reduces the conductivity of the electrodes and results in capacity decay and interior rate performance. Therefore, in order to obtain carbon based flexible electrodes with high performances, stable connection between high loading active materials and flexible carbon materials should be set up and the proportion of carbon materials should be minimized. The formation of chemical bonding between carbon materials and active substances and the development of lighter flexible carbon materials are effective strategies to improve the energy density and stability of flexible electrodes.

2.1.2. Polymer materials

Polymers tend to be extremely flexible, so it is a natural idea to introduce polymers into the electrodes to achieve high flexibility. In traditional LIBs, polymer materials such as PVDF and carboxymethylcellulose sodium (CMC) are added as binders in the slurry. The amount of the polymer binder is generally less than 10 wt% in traditional electrodes, so it is difficult to achieve high flexibility and endure the mechanical deformation of the electrodes in FLIBs. But with more insulating binder added to improve the flexibility, the conductivity and the energy density of the electrode will be decreased. Therefore, a feasible method for preparing a flexible electrode is to add controlled amounts of conductive polymer according to different situations.

Liu et al. developed two new kinds of conductive polymer binders, poly(1-pyrenebutyl methacrylate) (PBuPy) and poly(1-pyrenebutyl methacrylate-co-methacrylic acid) PBuPyMAA, in which butyl segments were synthetically incorporated between the methacrylate chain and the pyrene moiety [33]. Electrodes were prepared by mixing the graphene/silicon (Si) composite and the polymer binders together. The pyrene units increased the interaction between the polymer binders and the graphene sheets via the π-π stacking mechanism, and the insertion of the butyl segments enhanced the chain flexibility and increased the polymer-free volume. The conductive polymers helped to maintain the mechanical and electrical integrity of the electrode during charge/discharge processes when large volume change of silicon occurred. The electrode achieved an area capacity of over 5 mA h cm^{-2} and volumetric capacity of over 1700 Ah L^{-1} at a high current rate of 333 mA g^{-1}.

Some flexible polymers show reversible redox reaction with lithium ions and can be used as active materials of FLIBs. For example, Wei et al. synthesized a sulfur-linked carbonyl-based poly (2,5-dihydroxyl-1,4-benzoquinonyl sulfide) (PDHBQS) compounds as active materials for FLIBs (Fig. 3a) [34]. Flexible binder-free composites with single-walled CNTs (PDHBQS-SWCNTs) were fabricated by vacuum filtration. The cathode delivered a discharge capacity of 182 mA h g^{-1} (0.9 mA h cm^{-2}) at 50 mA g^{-1} with the potential window of 1.5 V–3.5 V, displayed a capacity of 75 mA h g^{-1} at a high current density of 5000 mA g^{-1}, and retained 89% of its initial capacity at 250 mA g^{-1} after 500 charge/discharge cycles. Flexible batteries based on the PDHBQS–SWCNTs cathode and the lithium foil anode exhibited good electrochemical performances under continuous bending. Flexible organic cathodes with 3,4,9,10-perylenetetracarboxylic diimide (PDI) as the active component, carbon black (CB) as the conductive agent, and thermoplastic polyurethane (TPU) as the elastomeric matrix were obtained (Fig. 3b) [35]. The cathodes displayed high mechanical/thermal stability, electrical conductivity, and electrolyte compatibility. The voltage-specific

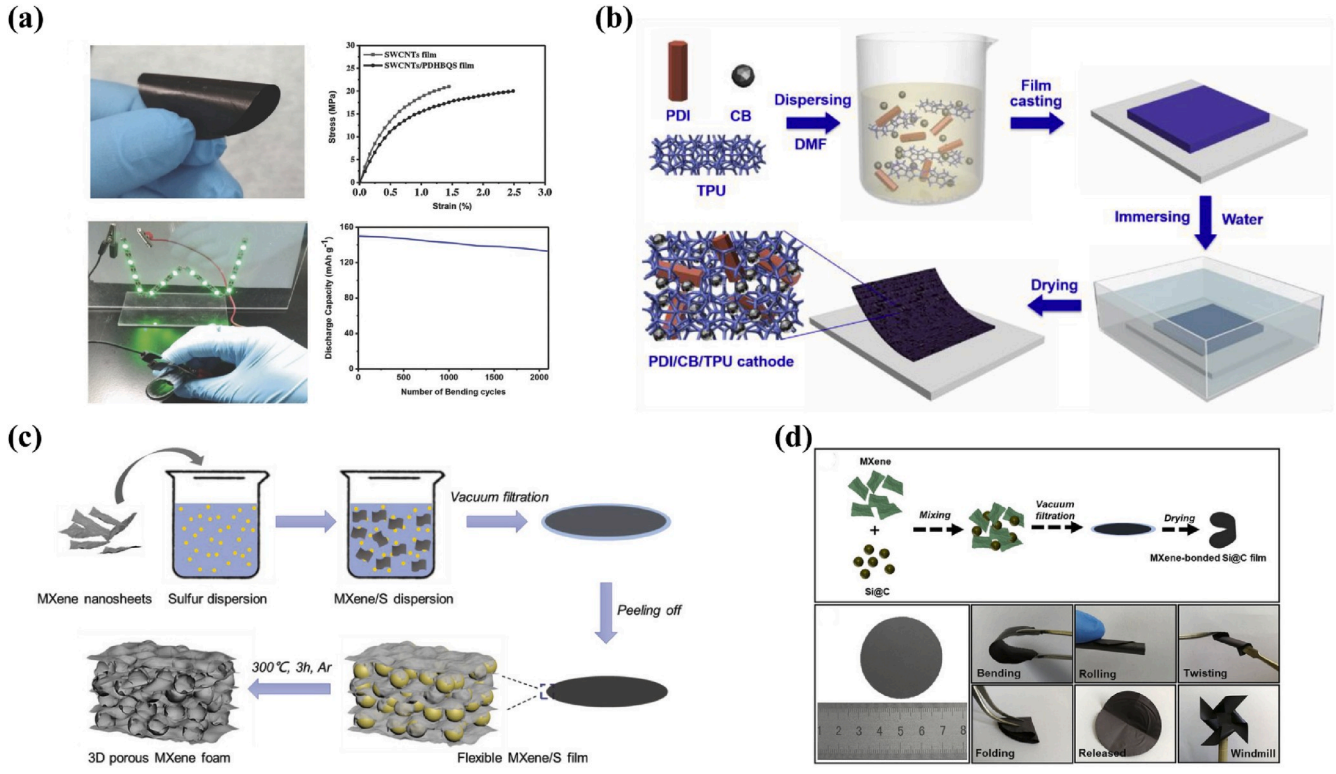

Fig. 3. (a) Photograph and stress-strain curve of a PDHBQS/SWCNTs film, photograph of a rolling battery, and the discharge capacities in 2000 bending cycles [34]. Reproduced with permission. Copyright 2017, Wiley-VCH. (b) The phase inversion fabrication processes of an integrated PDI/CB/TPU cathode [35]. Reproduced with permission. Copyright 2019, Elsevier, Inc. (c) Schematic of the preparation process of 3D Mxene foam [38]. Reproduced with permission. Copyright 2019, Wiley-VCH. (d) Schematic of the fabrication of a Mxene-based Si@C film and digital images showing its flexibility [39]. Reproduced with permission. Copyright 2019, Wiley-VCH.

capacity curves of the pouch cell under the flat and bent states showed almost the same performances, demonstrating the good flexibility of the pouch cell.

Polymers have the great advantages of extensibility, and there are a variety of polymers that can be applied as conductive binders or active materials in FLIBs. However, there are some shortcomings for polymers. For example, some polymers are not light-weight, resulting in low gravimetric energy density. Some conductive polymers are unstable under high voltage.

2.1.3. MXene materials

In addition to carbon materials and polymers, there are other materials that can be applied in flexible electrodes. MXene is a 2D material and has been widely applied in energy storage due to its high surface area, superior electrical conductivity, low lithium ion diffusion barrier, and good mechanical properties [36]. MXene can construct a conductive framework and integrate with other components in flexible electrodes.

Free-standing electrodes can be assembled by mixing MXene and electrode materials. Qian et al. fabricated a lightweight, flexible, and freestanding MXene/liquid metal paper by confining 3 °C GaInSnZn liquid metal in the MXene paper matrix [37]. MXene paper showed high electrical conductivity and good wettability with the liquid metal because of its rough surface. The composites delivered a capacity of 638.79 mA h g^{-1} at 20 mA g^{-1} and rate capacity of 404.47 mA h g^{-1} at 1000 mA g^{-1}, and showed better electrochemical performance than liquid metal coated Cu foil. 2D MXene suffers from aggregation and restacking of the 2D nanosheets, which limits its electrochemical performance. Xu et al. developed a 3D MXene foam with a porous structure via a simple sulfur-template method (Fig. 3c) [38]. The 3D porous architecture of the MXene foam offered massive active sites to enhance the lithium storage capacity and facilitated electrolyte infiltration for fast lithium ion transfer. As a result, the electrode based on 3D MXene foam displayed a specific capacity of 455.5 mA h g^{-1} at 50 mA g^{-1}, a rate capacity of 101 mA h g^{-1} at a current density of 18 A g^{-1}, and an outstanding long-term cycle stability of 220 mA h g^{-1} at 1 A g^{-1} after 3500 cycles. MXene can also be applied as binders for FLIBs. Xu et al. used 2D conductive MXene as a multifunctional binder to build a free-standing, flexible Si@C film [39]. MXene constructed a 3D conductive framework that provided space to buffer the volume change of Si@C nanoparticles and fast ion transport pathways (Fig. 3d). The electrodes displayed a stable performance with a capacity of 1040.7 mA h g^{-1} after 150 cycles at 420 mA g^{-1}. However, the electrodes exhibited

Table 1
Electrochemical performances of the batteries assembled by the flexible electrodes.

Materials		Details of Materials	Active materials	Electrochemical performance	Ref
Carbon Materials	CNT	SACNT as current collector	graphite	335 mA h g^{-1} (0.1 C) 326 mA h g^{-1} (2 C)	[14]
		HUCNM as current collector	$Li_4Ti_5O_{12}$/$LiCoO_2$	700 mA h 160 Wh kg^{-1}	[15]
		SACNT as free-standing electrode	$LiCoO_2$	151.4 mA h g^{-1} (0.1 C, 50 cycles) 137.4 mA h g^{-1} (2 C)	[16]
		SACNT as free-standing electrode	TiO_2	190 mA h g^{-1}/0.247 mA h cm^{-2} (1 C, 1.3 mg cm^{-2}) 100 mA h g^{-1} (60 C) 180 mA h g^{-1}/2.7 mA h cm^{-2} (0.2 C, 15 mg cm^{-2}	[17]
		CNT as free-standing electrode	Fe_2O_3	286 mA h g^{-1} (1 C, 400 cycles)	[18]
		CNT as free-standing electrode	MnO_2	796 mA h g^{-1}/0.955 mA h cm^{-2} (0.5 A g^{-1}, 1.2 mg cm^{-2}) 236 mA h g^{-1} (10 A g^{-1})	[19]
	Graphene	Graphene oxide sheets as free-standing electrode	MnO_2	920 mA h g^{-1}/2.576 mA h cm^{-2} (0.2 A g^{-1}, 2.8 mg cm^{-2}) 396 mA h g^{-1} (10 A g^{-1})	[21]
		Graphene oxide sheets as free-standing electrode	SnS_2	593 mA h g^{-1} (0.1 A g^{-1}, 200cycles) 134 mA h g^{-1} (2 A g^{-1})	[22]
		Graphene foam as free-standing electrode	$Li_4Ti_5O_{12}$/$LiFePO_4$	170 mA h g^{-1} (1 C, LTO/GF) 135 mA h g^{-1} (200 C, LTO/GF) 98 mA h g^{-1} (50C, LFP/GF)	[24]
		3D Graphene as free-standing electrode	Fe_2O_3	1129 mA h g^{-1} (0.2 A g^{-1}, 130 cycles) 534.2 mA h g^{-1} (5 A g^{-1})	[25]
		3D N-doped graphene as free-standing electrode	Ge	1220 mA h g^{-1} 800 mA h g^{-1} (40 C)	[26]
	CNF	CNF as free-standing electrode	$LiFePO_4$	133 mA h g^{-1}/2.66 mA h cm^{-2} (2 mA cm^{-2}, 20 mg cm^{-2}) 8.8 mA h cm^{-2}/30 mWh cm^{-2}/538 Wh L^{-1} (60 mg cm^{-2})	[29]
		CNF as free-standing electrode	Fe_2O_3/MoS_2	938 mA h g^{-1} (0.2 A g^{-1}, 300 cycles) 304 mA h g^{-1} (5.0 A g^{-1}) 6.46 mA h cm^{-2} (3 mA cm^{-2})	[30]
		CNF as free-standing electrode	Fe_2O_3	427 mA h g^{-1} (2 A g^{-1}) 183 mA h g^{-1} (10 A g^{-1}) 623 mA h g^{-1} (0.1 A g^{-1})	[31]
		CC and graphene as free-standing electrode	SnS_2	296,4 mA h g^{-1}/1.037 mA h cm^{-2} (0.5 A g^{-1}, 3.5 mg cm^{-2}, 150 cycles)	[32]
Polymers	Polymers	PBuPy and PBuPyMAA as binders	Si	5 mA h cm^{-2}/1700 Ah L^{-1} (0.333 A g^{-1})	[33]
		PDHBQS as active material	PDHBQS	182 mA h g^{-1}/0.9 mA h cm^{-2} (0.05 A g^{-1}) 75 mA h g^{-1}/0.47 mA h cm^{-2} (5 A g^{-1})	[34]
		3,4,9,10-PDI as active material TPU as the elastomeric matrix	PDI	124 mA h g^{-1} (0.05 A g^{-1}) 97 mA h g^{-1} (5 A g^{-1})	[35]
Mxene	Mxene	Mxene paper as free-standing electrode	GaInSnZn liquid metal	638.79 mA h g^{-1}/0.639 mA h cm^{-2}(0.02 A g^{-1}, 1 mg cm^{-2}) 404.47 mA h g^{-1} (1 A g^{-1})	[37]
		Mxene foam as free-standing electrode	pseudocapacitive mechanism/ lithium	455.5 mA h g^{-1}/0.456 mA h cm^{-2} (0.05 A g^{-1}, 1 mg cm^{-2}) 101 mA h g^{-1} (18 A g^{-1})	[38]
		Mxene as binder	Si	1040.7 mA h g^{-1}/1.249 mA h cm^{-2} (0.42 A g^{-1}, 1.2 mg cm^{-2}, 150 cycles) 553 mA h g^{-1} (8.4 A g^{-1})	[39]
		Mxene as active material	Ti_3C_2	170mAhg^{-1} (0.04 Ag^{-1}) 114 mA h g^{-1} (2 A g^{-1}) 59 Wh kg^{-1}	[40]

a lower coulombic efficiency (73.0%) than that of the CMC-bonded Si@C electrode (80.2%) and PVDF-bonded Si@C electrode (73.9%). MXene can also work as active material, as reported by Geng et al. [40]. A flexible, lightweight electrode for quasi-solid-state batteries was developed by stacking molecularly coupled titania sheets (Ti_3C_2) with CNTs. The electrode demonstrated high flexibility and could be repeatedly folded into any shapes. The high conductivity, high interface of the active atoms, and pathways for ion intercalation resulted in improved electrochemical performance. The electrode displayed discharge capacity of 170 mA h g^{-1} at 40 mA g^{-1}, good rate capability of 114 mA h g^{-1} at a current density of 2000 mA g^{-1}, and excellent long-term cycling stability with a 93.1% retention rate after 1000 cycles at 1000 mA g^{-1}. Moreover, a full quasi-solid-state battery with high flexibility displayed a power density of 1412 W kg^{-1} while maintaining an energy density of 59 Wh kg^{-1}.

In summary, the preparation of flexible electrodes using carbon materials, polymers, and MXene is reviewed in this section, and the electrochemical performances of these electrodes based on these materials are shown in Table 1. There are some common characteristics of these materials by analyzing their performances: (i) These materials have high conductivity and good contact with the active materials to facilitate fast electron transfer. (ii) These materials can accommodate the volume change of the active materials and the repeated mechanical deformation of the electrodes, leading to structure integrity. (iii) These materials can create channels for effective ion transport. (iv) These materials show thermal and chemical stability during the charge/discharge processes. In order to develop high-performance flexible electrodes of FLIBs, the electrode materials need to possess these characteristics. Furthermore, combining several materials together to develop flexible electrodes is also a solution.

2.2. Flexible electrolyte

Electrolyte is another crucial component in FLIBs. The electrolyte used in FLIBs should have the following characteristics: (i) It should have high ionic conductivity and electronic insulation. (ii) The electrolyte itself is flexible. (iii) There is no side reaction between the electrolyte and cathode/anode. (iv) The electrochemical window of the electrolyte is within the appropriate range. (v) It can maintain good contact with active materials, and has small interface resistance, even under mechanical deformation. Liquid organic electrolyte commonly used in traditional LIBs has the advantages of high ionic conductivity, wide electrochemical window, good chemical stability, and sufficient contact with electrodes. However, the liquid organic electrolyte has safety issues. Taking $LiPF_6$, the most commonly used lithium salt in liquid electrolyte, as an example, its thermal stability and chemical stability are poor, and it easily reacts with a trace amount of water presented in the electrolyte to generate highly reactive PF_5, causing the decomposition of organic solvents. The decomposition products even contain some inflammable gases, and these problems will become more serious as the battery temperature rises during the charge and discharge processes [41]. Moreover, the liquid electrolyte cannot prevent the growth of lithium dendrites, which penetrate the separator and thus lead to a short circuit or even battery explosion. For FLIBs, the liquid electrolyte is prone to flow during mechanical deformation, which results in an unstable battery system. Alternatively, solid and gel electrolytes are ideal options for use in FLIBs.

Solid electrolyte refers to a novel liquid-free electrolyte that can replace the liquid electrolyte and separator. Inorganic solid electrolyte and polymer electrolyte are commonly used solid electrolytes. Inorganic solid electrolytes including oxides, sulfides, and glass ceramics, etc. [42–45] can provide fast migration channels for lithium ions through their point defects or special crystal structure, and thus generally have extremely high ionic conductivity. However, these materials have a large interface contact resistance between the electrolyte and electrodes and are highly rigid, making them difficult to use in FLIBs. Polymer electrolyte is an ideal choice for FLIBs because of its flexibility and strong interface compatibility. However, the ionic conductivity and electrochemical stability of polymer materials are inferior to those of liquid electrolytes and inorganic solid electrolytes. Therefore, polymer solid electrolytes are composited with inorganic solid electrolytes and liquid electrolytes to form inorganic-organic composite solid polymer electrolytes and gel polymer electrolytes, which possess high flexibility, good interfacial characteristics, and greatly improved ionic conductivity and electrochemical stability. At present, inorganic-organic composite solid polymer electrolytes and gel polymer electrolytes are the most commonly used flexible electrolytes in FLIBs. In this paper, the advantages and disadvantages of commonly used polymer materials are summarized first, and the research routes of improving ionic conductivity and electrochemical stability of solid and gel electrolytes based on polymers are reviewed.

2.2.1. Commonly used polymer materials

Commonly used polymer electrolyte materials mainly include poly (ethylene oxide) (PEO), poly(ester), nitrile, and PVDF. PEO was discovered as an ionic conductor in 1973. A linear ether oxygen (EO) group in the repeating structural unit of PEO makes it suitable for flexible polymer solid electrolytes, and its flexible nature also ensures good contact between the electrolyte and the active material. The EO groups can form complexes with many lithium salts, such as LiBr, LiCl, LiI, LiSCN, $LiBF_4$, $LiCF_3SO_3$, LiTFSI, etc., and the migration process of lithium ions in PEO-based polymer electrolytes can be considered as the coordination and dissociation process of lithium ions and EO groups. Under electric field, the migration ions and the EO group continuously undergo the coordination-dissociation process, and the rapid migration is achieved through the segmental motion of local PEOs. However, PEO is a thermoplastic material, and there are many crystalline regions that lead to limited movement of the segments, thus reducing the ionic conductivity (10^{-7} S cm^{-1} at room temperature). Moreover, the electrochemical window of PEO is narrow, and oxidation occurs at about 3.8 V [46], limiting the application of PEO in high-voltage FLIBs.

In order to solve the problem of the narrow electrochemical window of PEO, Goodenough et al. designed a double-layer polymer electrolyte for high-voltage LIBs. As shown in Fig. 4a, the PEO-LiTFSI layer was in contact with the anode and the poly(N-methyl-malonic amide) (PMA)-LiTFSI layer was in contact with the cathode. The double-layer electrolyte constructed in this way had better electrochemical stability, could work stably at 4 V, and maintained excellent ionic conductivity even after long cycle life [47]. Many researchers have also tried to overcome the low ionic conductivity in PEO through some unique structural designs or processing methods. Yi et al. used nanoporous polyimide (PI) and PEO/LiTFSI to prepare an ultra-light flexible PI/PEO/LiTFSI solid electrolyte with a thickness of only 8.6 μm, which had high ionic conductivity (2.3×10^{-4} S cm^{-1} at 30 °C) [48]. All-solid-state FLIBs fabricated with PI/PEO/LiTFSI solid electrolyte showed good cycling performance in 200 cycles at 0.5 C at 60 °C and withstood abuse tests such as bending, cutting, and nail penetration.

The main characteristic groups of poly(ester) are ester groups with strong polarity, which can effectively dissolve alkali metal salts and reduce the tendency of ion aggregation. Carbonate materials such as poly(ethylene carbonate) (PEC) [49], poly(trimethylene carbonate) (PTMC) [50] and PPC [51] have been widely studied because the polar carbonate groups can improve the dielectric constant and ionic conductivity. Jannasch's team prepared poly(ethylene oxide-co-ethylene carbonate) (PEO-EC) electrolyte by anionic ring-opening polymerization. The incorporated polar carbonate groups into polyether chains not only reduced the crystallinity of the polymer but also increased the relative dielectric constant [52]. In 2015, Mindemark et al. prepared a copolymer of trimethylene carbonate (TMC) and ε-caprolactone (CL), as shown in Fig. 4b. By adjusting the ratio of TMC and CL, the ionic conductivity reached 1.6×10^{-5} S cm^{-1} at 60 °C [53].

As a biodegradable material, PPC is alternately bonded by

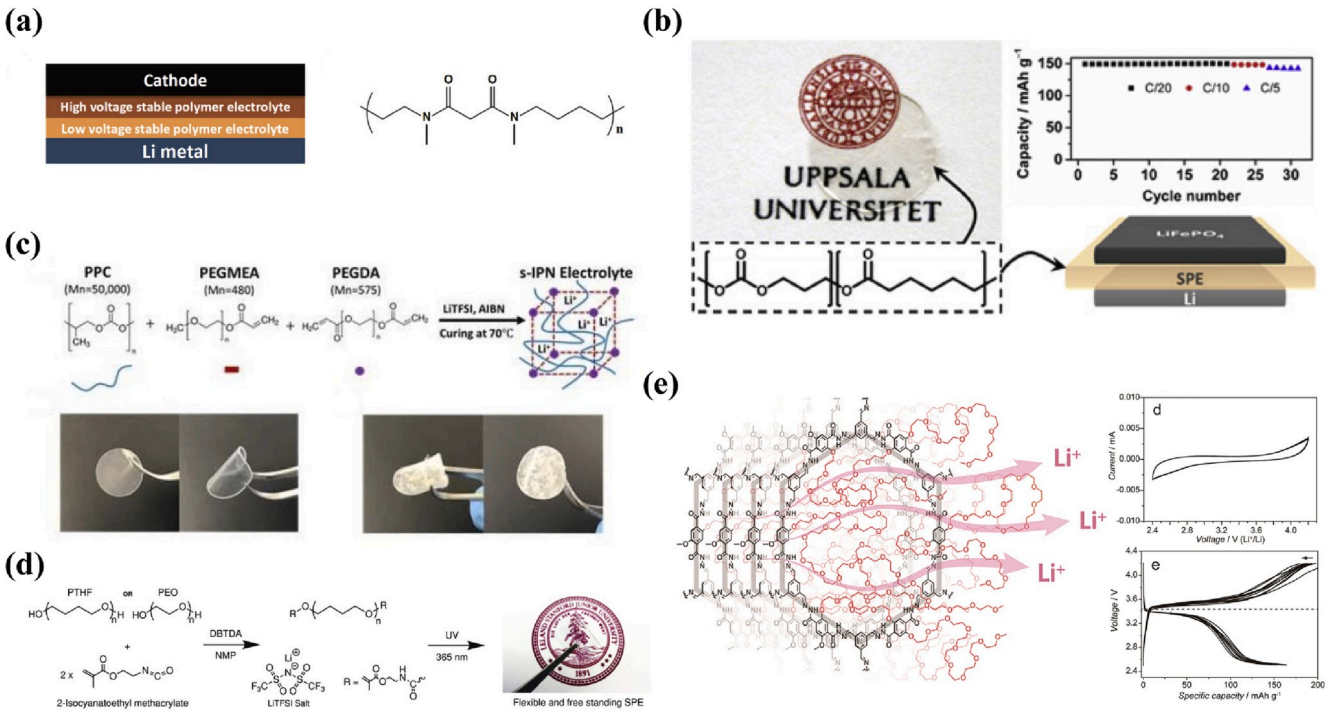

Fig. 4. (a) Stacking model of PEO/PMA dual layer electrolyte in an all-solid-state cell [47]. Reproduced with permission. Copyright 2018, Wiley-VCH. (b) Morphology and performance of TMC-εCL copolymer [53]. Reproduced with permission. Copyright 2015, Elsevier, Inc. (c) Illustration of the preparation and structure of s-IPN electrolyte [54]. Reproduced with permission. Copyright 2005, The Electrochemical Society. (d) Synthesis route to prepare xPTHF electrolyte [59]. Reproduced with permission. Copyright 2018, Wiley-VCH. (e) Lithium ion transport mechanism and electrochemical properties of COF [60]. Reproduced with permission. Copyright 2018, American Chemical Society.

heterogeneous propylene oxide and carbon dioxide. PPC has attracted a lot of attention due to its amorphous, low-cost, and environmentally friendly features. Based on the chemical structure of PPC similar to conventional carbonate-based liquid electrolyte, PPC is considered to have excellent solubility of lithium salts and excellent compatibility with lithium metal interface. As shown in Fig. 4c, Yang et al. introduced a semi-interpenetrating polymer network (s-IPN) by mixing PPC, poly (ethylene glycol) methylether acrylate (PEGMEA), poly(ethylene glycol) diacrylate (PEGDA), and LiTFSI. The PPC performs as film forming agent, and the ionic conductivity of the flexible electrolyte reached 5×10^{-6} S cm^{-1} at ambient temperature [54].

In recent years, succinitrile (SN) electrolytes containing polar electron-absorbing nitrile groups with high dielectric constant and wide electrochemical window have attracted more attentions due to their excellent electrochemical properties and good compatibility with lithium metal [55]. SN is a low molecular weight plastic crystal that accepts electrons with a high oxidation potential, and its dielectric constant of 55 at 25 °C indicates its ability to dissolve a variety of lithium salts. Armand et al. found that after doping 5 mol% LiTFSI in SN, the ion conductivity could reach 3×10^{-3} S cm^{-1}. Moreover, the plasticity of SN is similar to that of polymer electrolyte, which indicates that the SN based electrolyte can adapt to the volume change of active materials and achieve the goal of long cycle of lithium battery [56].

Polyacrylonitrile (PAN) is also a widely studied material with nitrile groups. Similar to the PEO material, PAN has a low ionic conductivity (10^{-7} S cm^{-1}) at room temperature and a narrow electrochemical window (<3.7 V), making it difficult to apply in polymer electrolytes alone. The ionic conductivity of PAN could be effectively improved by grafting, blocking, cross-linking and other means to reduce the crystallinity of PAN fragments. Beyond that, PAN composites with excellent ionic conductivity and electrochemical stability can be obtained by adding inorganic fillers or liquid plasticizers to form a gel-like polymer electrolyte [57].

PVDF has a high dielectric constant (~8.4), which is beneficial to the dissociation of lithium salts. At the same time, PVDF has good mechanical properties, wear and corrosion resistance, hydrophobicity, and excellent processing performance, making it more suitable for LIBs. It is also an ideal material for preparing polymer electrolyte. However, PVDF has poor ionic conductivity due to its ordered structure and high molecular symmetry. Researchers generally reduce the crystallinity through blending, copolymerizing, and crosslinking, to obtain gel polymer electrolyte with high ionic conductivity. To improve the electrochemical stability and ionic conductivity, Liang et al. developed a poly (vinylidene fluoride)/poly (methyl methacrylate) (PVDF/PMMA) composite fibrous membranes as the separator of FLIBs by electrospinning [58]. At room temperature, the maximum ionic conductivity was 2.54×10^{-3} S cm^{-1}, and the electrochemical window reached 5.0 V.

The properties of commonly used polymer materials are summarized in Table 2. The fatal problem faced by the polymers is still the low ionic conductivity that causes serious polarization and poor rate performance of batteries. Various methods such as cross-linking, copolymerizing, blending, organic-inorganic composite, and preparation of gel electrolyte are effective to solve this problem. The related work of organic-inorganic composites and preparation of gel electrolytes are explained

Table 2
Electrochemical properties of different polymers.

Polymer categories	Polymer materials	Ionic conductivity (S cm^{-1})	Oxidation potential (V)
Poly(ethylene oxide)	PEO	10^{-7} [61]	3.8 [46]
Poly(ester)	PEC	10^{-4} [62]	4.5 [61]
	PTMC	10^{-5} [63]	5.0 [64]
	PPC	10^{-4} [65]	4.6 [65]
Nitrile	SN	10^{-3} [56]	6.0 [56]
	PAN	10^{-7}[66]	3.7 [67]
Poly(vinylidene fluoride)	PVDF	10^{-4} [68]	4.3 [57]

in detail below.

In addition to the commonly used polymers mentioned above, some novel polymer-based materials are emerging. Yi and Bao et al. introduced cross-linked poly(tetrahydrofuran) (xPTHF) as a promising polymer matrix for "beyond PEO" solid polymer electrolytes (Fig. 4d). The cross-linking procedure created thermally stable and mechanically robust membranes for use in LIBs. The lower spatial concentration of oxygen atoms in the xPTHF backbone resulted in loosened O–Li^+ coordination that enhanced ion transport [59].

Covalent organic framework (COF) is an emerging class of crystalline organic polymers with periodic structure and tunable functionality, which exhibit potential as a unique ion conductor/transporter. Kitagawa and Horike et al. used COF as an organic solid electrolyte medium and applied a bottom-up self-assembly method to obtain covalently networked flexible bulky glassy polymer electrolyte, which dissolved lithium ion by segmental motion in a rigid two-dimensional structure to achieve rapid lithium ion transport (Fig. 4e) [60].

2.2.2. *Flexible composite solid polymer electrolytes*

As for FLIBs, high flexibility is the basic requirement of electrolyte. However, pure polymer electrolyte has low ionic conductivity and poor electrochemical stability, which limit its application. In 1998, Scrosati et al. added nano-sized TiO_2 and Al_2O_3 ceramic powders into the PEO matrix, which increased the ionic conductivity by 1–2 orders of magnitude and enhanced the mechanical properties of the polymer matrix [69]. The organic and inorganic composite electrolyte aroused the interest of researchers. Yi et al. prepared a AAO/Polymer composite electrolyte using surface-modified ceramics and polymer (Fig. 5a), and achieved an overall ionic conductivity of 5.82×10^{-4} S cm^{-1} at room temperature. Moreover, the enhanced ion conduction behavior at the ceramic/polymer interface was confirmed by experiments for the first time, and the interfacial ionic conductivity was calculated to be higher than 10^{-3} S cm^{-1} even at 0 °C [70]. Nowadays, these inorganic fillers not only include oxide nanoparticles, but also inorganic solid electrolyte, MOF, ceramic, etc. and the morphology of inorganic fillers are also diverse, including nanoparticles, aerogels, porous membranes. This kind of organic and inorganic composite solid electrolyte has both the flexibility of polymer solid electrolyte and good interface contact, as well as the improvement of ionic conductivity after adding inorganic fillers, which are crucial for FLIBs.

As shown in Fig. 5b, by constructing a 3D nanostructured garnet skeleton as an inorganic and organic composite electrolyte, the ionic conductivity of the electrolyte was significantly improved [71]. At the same time, its electrochemical stability, thermal stability, and stability to the interface with lithium metal were also enhanced. This 3D skeleton design provided an effective strategy for developing the next generation of high-performance composite polymer electrolytes for lithium batteries. Nan et al. used $Li_{6.75}La_3Zr_{1.75}Ta_{0.25}O_{12}$ (LLZTO) ceramics to trigger structural modification of PVDF polymer electrolytes (Fig. 5c), and found that the interaction between PVDF matrix, lithium salt, and LLZTO filler activated by partially modified PVDF chains significantly improved the ion conductivity of flexible electrolyte membranes [72].

Hu et al. designed a flexible garnet-based electrolyte membrane consisted of c-LLZO wafers and styrene-butadiene copolymer (SBC) grout (Fig. 5d) [73]. The flexible electrolyte membrane body was a garnet ceramic block, and the slit was connected by a SBC, which effectively suppressed the strain energy below the fracture toughness of the garnet solid electrolyte, thereby eliminating random cracks. The film had a high ductility of up to 220% and an ultimate tensile strength of 5.12 MPa. The method is compatible with the manufacturing industry technology and has great application significance.

Goodenough et al. prepared a high Li^+ mobility inorganic and

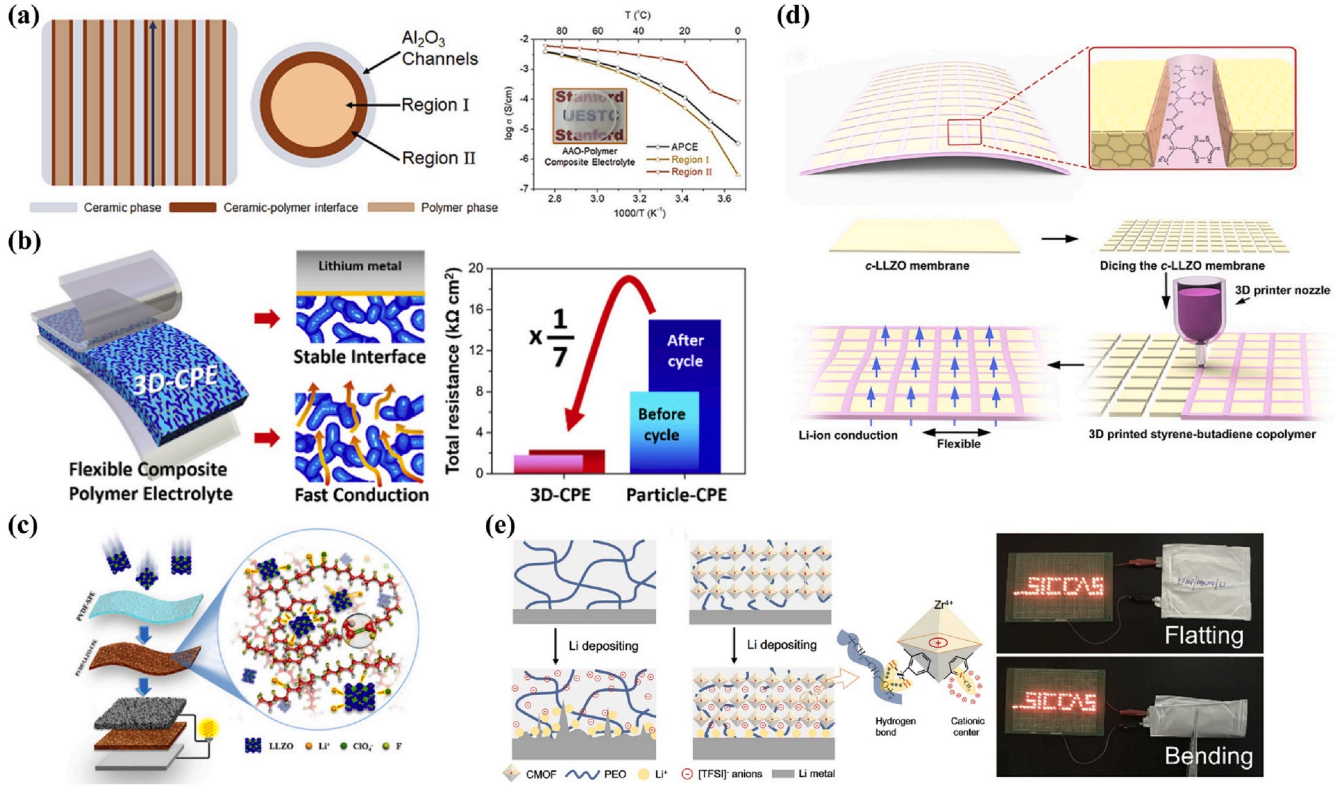

Fig. 5. (a) Structure and performance of AAO-polymer composite electrolyte [70]. Reproduced with permission. Copyright 2018, American Chemical Society. (b) Schematic of 3D garnet framework based composite polymer electrolyte [71]. Reproduced with permission. Copyright 2018, Elsevier, Inc. (c) Structures of PVDF/LLZTO-CPEs [72]. Reproduced with permission. Copyright 2017, American Chemical Society. (d) Schematic of the fabrication of a flexible c-LLZO SSE membrane [73]. Reproduced with permission. Copyright 2019, American Chemical Society. (e) Schematic of FLIBs and Li deposition behavior with PEO(LiTFSI) electrolyte and anion-immobilized P@CMOF electrolyte [77]. Reproduced with permission. Copyright 2019, Elsevier, Inc.

organic composite solid electrolyte, which was composed of a garnet electrolyte ($Li_{6.5}La_3Zr_{1.5}Ta_{0.5}O_{12}$) coated with a conductive polymer PEO-Lithium poly(acrylamide-2-methyl-1-propane-sulfonate) (PAS) [74]. PEO-PAS separated the garnet electrolyte from the lithium metal to inhibit lithium dendrite nucleation. At the same time, the introduction of the lithium ion conductor coating not only exhibited good adhesion to the ceramic electrolyte and lithium metal but also provided a uniform interface. The first coulombic efficiency of the all-solid-state lithium metal battery assembled with PCSSE was as high as 97%, and the subsequent cycle efficiency maintained at 99.9–100%.

Metal-organic frameworks (MOFs), a compound composed of an inorganic metal center and an organic ligand, are a class of crystalline porous materials with a periodic network structure. Since the first addition of lithium isopropoxide to Mg_2(dobdc) (dobdc^{4-} = 1,4-dioxido-2,5-benzenedicarboxylate) as a solid electrolyte by Long et al. [75], MOFs have been widely used in solid electrolytes for lithium batteries. Guo et al. uniformly dispersed UIO-66/Li-containing ionic liquid (Li-IL) as a filler in an anhydrous acetonitrile solution of PEO and LiTFSI. By dissolving the cast film, a self-supporting PEO-n-UIO solid electrolyte was obtained. When 40% of UIO/Li-IL was added, the ionic conductivity of PEO-n-UIO solid electrolyte increased by 37 times at 30 °C, which was 1.3×10^{-4} S cm^{-1} [76]. Ge et al. used UiO-66 (Zr-BDC MOF) as a raw material to synthesize a novel cationic MOF (CMOF) material by nucleophilic substitution of grafted pyridine N (Fig. 5e). The specific surface area of the material is as high as 1082 m^2 g^{-1}. The anion is fixed by the electrostatic action of the charge carrier. Subsequently, CMOF was dispersed in PEO/LiTFSI electrolyte and P@CMOF composite solid electrolyte was prepared by a hot pressing method. Its ionic conductivity was an order of magnitude higher than that of pure PEO. Using $LiFe_{0.15}Mn_{0.85}PO_4$ as the cathode and P@CMOF as the electrolyte, a flexible pouch cell was assembled. The initial coulombic efficiency of the cell at 9 C was 94.1%, and the capacity retention after 100 cycles was 81.2% [77].

To summarize, how to design molecular structures for fast ion conduction/transport in the solid-state has always been a significant challenge for flexible polymers. All kinds of polymers have distinct advantages and disadvantages, and they are rarely used alone. Inorganic-organic composite is an effective means to utilize the flexibility of polymer and greatly improve the ionic conductivity. Moreover, through the selection of different inorganic substances, flexible electrolytes for use in FLIBs can be designed.

2.2.3. Flexible gel polymer electrolytes

In addition to the above-mentioned preparation of composite solid polymer electrolytes by compounding polymers with inorganic substances, gel electrolyte is another way to obtain flexible electrolytes. Polymer molecules are connected under certain conditions to form a spatial network structure in which the liquid dispersion is swollen, and the gelatinous substances containing both solid and liquid form the gels. Feullade and Perche first proposed gel electrolyte in 1975 [78], which has been developed rapidly in the past 40 years. Gel electrolyte generally contains polymer matrix, lithium salt, and plasticizer. The polymer matrix in the electrolyte has a certain mechanical strength. The plasticizer can reduce the crystallinity of the polymer matrix to improve the ionic conductance of the polymer. Furthermore, the plasticizer is mostly composed of lithium-ion conductor such as liquid electrolyte, which can provide express channels for of a large number of ions. Therefore, the ionic conductivity of the gel electrolyte is close to that of liquid electrolyte. Nowadays, gel electrolytes for use in FLIBs can be obtained by plasticizer added gelation or in-situ gelation.

2.2.3.1. Plasticizer added gelation. The simplest way to prepare gel electrolyte is to absorb liquid electrolyte by polymer matrix commonly used in LIBs. To obtain flexible gel electrolyte, the polymer matrix needs to have the following features: (i) The polymer matrix has great absorption and retention of liquid; (ii) The polymer matrix remains flexible after absorbing the plasticizer; (iii) The polymer matrix does not react with the plasticizer. The commonly used polymer matrix in gel electrolytes mainly includes PAN, PEO, PMMA, PVDF and their corresponding derivatives.

PEO was the first to be studied. The addition of organic plasticizer in PEO can effectively increase the distance between the molecular chain segments in the polymer, reduce the ordering of the molecular chain arrangement, weaken the interaction between the chain segments, reduce the crystallinity, and increase the amorphous components. Therefore, the ionic conductivity is greatly improved. For example, after adding EC, DEC, PC and other plasticizers into PEO-$LiBF_4$ system, the ionic conductivity of the gel electrolyte was equivalent to that of the liquid electrolyte [79].

Gel electrolyte composed of PAN, lithium salt, and solvent has high ionic conductivity (10^{-3} S cm^{-1}). The complexing force between the PAN polymer chain segment and lithium ions is weaker than that of PEO, leading to larger lithium-ion migration number of PAN gel electrolyte. For some large anionic lithium salts, the lithium-ion migration number could be increased to 0.7 [80]. The force between the chain segment of the PAN polymer and the liquid electrolyte was not strong, and the retention of liquid was poor [81]. In addition, PAN gel electrolyte was not compatible with lithium metal, and it was easy to form an unstable passivation layer, which affected the cycle performance of the battery, and even had a safety hazard [82–84].

PVDF has a strong electron-absorbing halohydrocabron group, which becomes a polymer matrix material with high anionic stability. After PVDF was plasticized by LiTFSI dissolved in PC, the ionic conductivity was 1.74×10^{-3} S cm^{-1} at 30 °C, and the oxidation potential of Li^+/Li was 3.9–4.3 V. However, because the halohydrocabron group in PVDF gel polymer molecular chain reacted with lithium metal under certain conditions and was reduced to LiF and F, the interface stability between fluoropolymer and lithium metal was poor [85]. In addition, PVDF had a high crystallinity and contained both crystalline and non-crystalline phases. Liquid electrolyte wetting was mainly completed in the non-crystalline phase, and the existing crystalline phase could not store the electrolyte, resulting in a phase separation between the non-crystalline phase and electrolyte, impeding the migration of lithium ions, and affecting the circulation and performance of the battery. In recent years, the derivative poly (vinylidene fluoride)-hexafluoropropylene (PVDF-HFP) based on PVDF has attracted the attentions of many scholars. The amorphous phase to HFP lowered the crystallinity of the polymer main body, and helped the polymer substrate adsorb more plasticizer [86–90].

The electrochemical properties of gel electrolytes are related to not only the polymer materials, but also the selection of plasticizer. Plasticizers used in gel electrolytes should have high electrochemical stability and good compatibility with polymer matrix. Plasticizers used in the gel electrolyte can be divided into liquid electrolyte, ionic liquid (IL), and aqueous solution.

Small-molecule organic solvents commonly used in traditional electrolytes include dimethyl carbonate (DMC), methyl ethyl carbonate (EMC), diethyl carbonate (DEC), ethylene carbonate (EC), polycarbonate (PC). Partly or wholly fluorinated carbonates such as fluorinated carbonates (FEC) can be used as plasticizers. Lithium salts dissolved in these solvents are mainly $LiPF_6$, $LiClO_4$, $LiBF_4$, LiFSI, LiTFSI, LiBOB, LiDFOB, etc. When the plasticizer infiltrates the polymer matrix film, the crystallinity of the polymer is reduced and the glass conversion temperature of the system is also lowered. Therefore, the activity of the polymer chain segment and the dissociation degree of lithium ions are greatly improved in the gel electrolyte system. As shown in Fig. 6a, Tang and Zhou et al. developed a gel electrolyte with 3D cross-linked porous network structure formed by PVDF-HFP, PEO, and GO through weak interactions such as hydrogen bond. The lithium salts and plasticizers were $LiPF_6$ and a mixture of EMC and vinylene carbonate (VC), respectively. The battery had good flexibility and high ionic

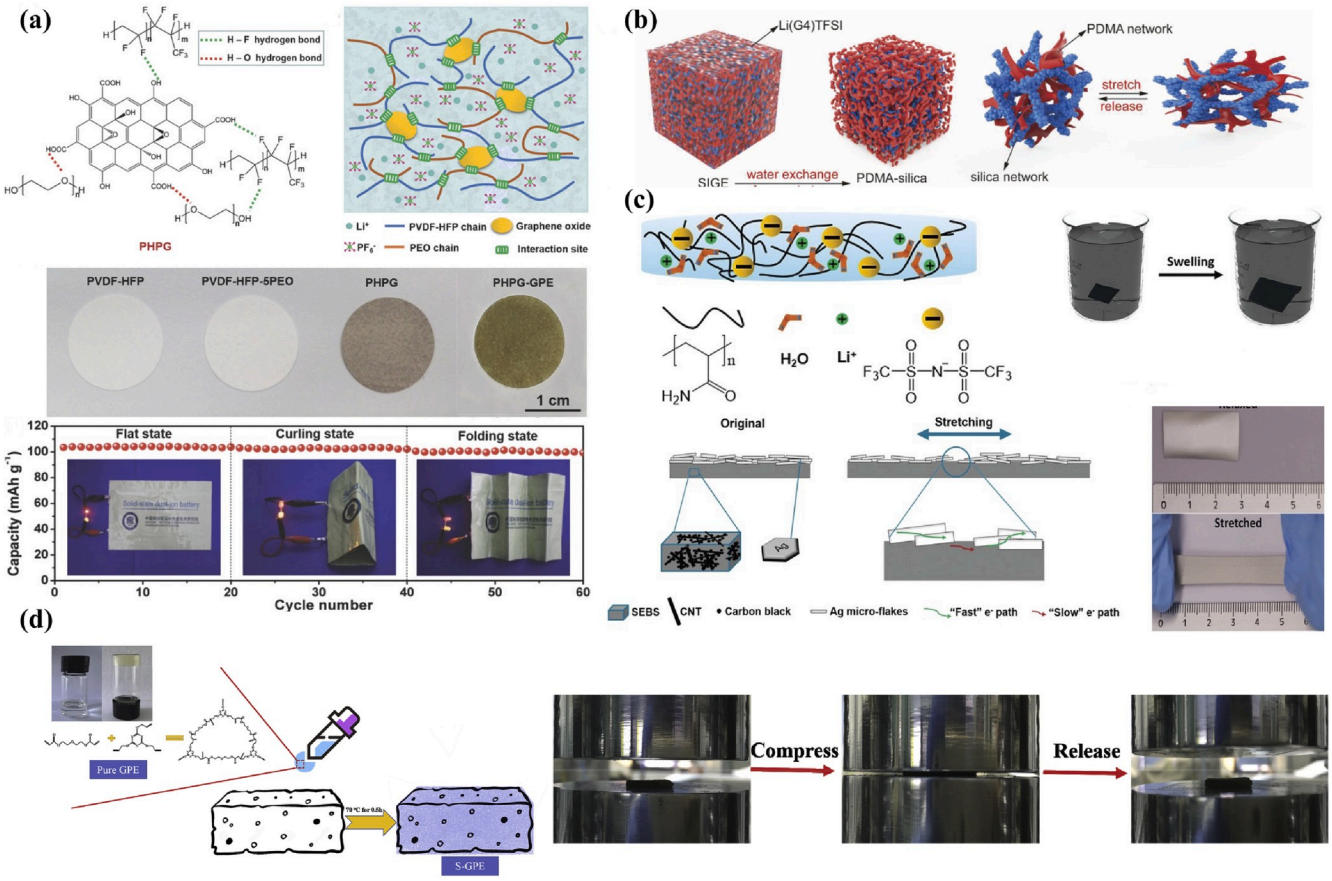

Fig. 6. (a) Schematic of the intermolecular hydrogen binding effect and 3D porous polymer network of PHPG, and cycling performance of the flexible PHPG-DIB [91]. Reproduced with permission. Copyright 2018, Wiley-VCH. (b) Schematic of the DN structures [95]. Reproduced with permission. Copyright 2019, Wiley-VCH. (c) Illustration of the preparation process of PAM-WiS membrane and its stretchability [96]. Reproduced with permission. Copyright 2019, Wiley-VCH. (d) The schematic of preparation for the GPE and S-GPE and the compressibility of S-GPE$_2$ [98]. Reproduced with permission. Copyright 2019, Elsevier, Inc.

conductivity (2.1×10^{-3} S cm^{-1}) [91].

ILs are a class of molten salts with low melting points composed of anionic and cationic only, also known as room temperature molten salt. Due to their low vapor pressure, high flash point, nonflammablility, good thermal stability, high conductivity, and diversity of structural design, ILs have aroused extensive interest of researchers. There are many types of ILs, which are generally classified according to different cations, mainly including quaternary ammonium salts, quaternary phosphorus salts, quaternary sulfur salts, and azacyclic types. Azacyclic ILs have been studied the most, including imidazoles, pyridines, and pyrrole types. Compared with traditional liquid electrolyte plasticizer, azacyclic ILs have the following advantages: (i) They can conduct electricity by themselves, which can significantly improve ionic conductivity of polymer electrolyte. (ii) They possess high thermal decomposition temperature and nonflammablility, which can avoid safety problems of the solvent that burns easily in the traditional organic electrolyte. (iii) They have high chemical stability and wide electrochemical stability window, which can be used in high-voltage batteries. (iv) They are non-volatile, environmentally friendly, and pollution-free.

The gel electrolyte prepared by blending ILs with the polymer matrix and lithium salt is called ion gel polymer electrolytes (IGPEs). The earliest IGPE was prepared by Carlin et al. by blending 1-ethyl-3-methylimelate IL with PVDF-HFP [92], which had high ionic conductivity at room temperature. IGPE has the advantages of both ionic liquid and flexible polymer electrolytes, and the problems of solvent volatilization and liquid leakage can be avoided, obtaining batteries with high safety and stability. IL as plasticizer could reduce the glass transition temperature of polymer and made the gel more elastic [93,94]. For instance, Hu et al. reported a solvated IL gel electrolyte with organic-inorganic dual network structure (Fig. 6b). This electrolyte combined the advantages of dual network structure and solvated IL, and had excellent mechanical properties. It could withstand compression deformation of 80 MPa and returned to its original state. It had a good application prospect in the field of high safety and flexible energy storage devices [95].

In recent years, with the improvement of safety and environmental protection requirements for batteries, aqueous electrolyte has begun to get more attention. Compared with organic electrolyte, aqueous electrolyte is nontoxic, nonflammable, and low-cost. Moreover, the ion conductivity of the aqueous electrolyte is two orders of magnitude higher than the organic electrolyte, which greatly accelerates the reaction dynamic of LIBs and makes the application of super thick electrodes possible. However, the narrow electrochemical window of aqueous electrolyte is still a biggest defect, limiting its application in traditional electrode materials of LIBs, such as $LiCoO_2$/graphite. In 1994, Dahn et al. firstly proposed a system with VO_2 as the anode and $LiMn_2O_4$ as the cathode, which possessed a theoretical energy density of up to 75 Wh kg^{-1}. Since then, many studies have been conducted on the materials of electrode and aqueous electrolyte to improve the performance of LIBs, and how to make flexible aqueous LIBs has become a brand new research field.

Niederberger et al. assembled a highly elastic thin-film full battery using a polyacrylamide (PAM) hydrogel composite "water-in-salt" (WiS) aqueous electrolyte and flexible electrodes prepared with $LiMn_2O_4$ and V_2O_5 material coated on a composite polymer current collector with an internal carbon network (Fig. 6c). Under 50% tensile strain, it maintained a capacity of 28 mA h g^{-1}, and the average energy density was 20

Wh kg^{-1} after 50 cycles at a current density of 120 mA g^{-1}, which made it promising to be applied in flexible retractable solid-state pouch cells [96].

2.2.3.2. In situ gelation. In addition to the traditional method of preparing polymer matrix first and then adding plasticizer to obtain gel after swelling, in-situ gelation technology has recently become an emerging means to improve the performance of liquid electrolyte. The in-situ gelation method is to design several liquids with special functional groups that can spontaneously polymerize to obtain gel electrolytes under the condition of initiators, light, heat, etc. This method greatly simplifies the preparation of the gel electrolyte and reduces the introduction of impurities in the process of material preparation and battery assembly.

Li and Guo et al. developed a new strategy to convert traditional etheryl 1,3-dioxopentyl ring (DOL) and 1,2-dimethoxyethane (DME) liquid electrolyte into novel quasi-solid gel electrolyte by adding commercial $LiPF_6$. Among them, the cationic open-loop polymerization between $LiPF_6$ and DOL was first discovered and applied to the lithium secondary battery system. On this premise, the new gel electrolyte has been successfully applied to a series of lithium metal batteries containing sulfur, $LiFePO_4$ and $LiNi_{0.6}Co_{0.2}Mn_{0.2}O_2$ (NCM622) cathode, showing excellent universality and commercialization prospects [97].

As shown in Fig. 6d, Chen et al. prepared a sponge gel polymer electrolyte by in-situ gelation of precursor solution-soaked (1,2-diacrylyl ethane, 2,4,6-triallyloxy-1,3,5-triazine and $LiPF_6$ electrolyte) commercial sponge [98]. The prepared gel electrolyte exhibited a remarkable ionic conductivity (1.08 mS cm^{-1}) even larger than that of liquid electrolyte infiltrated-Celgard 2400 (0.95 mS cm^{-1}) and could resist compression deformation.

3. New battery structures and assembly methods

The typical structures of commercial LIBs are mainly cylindrical

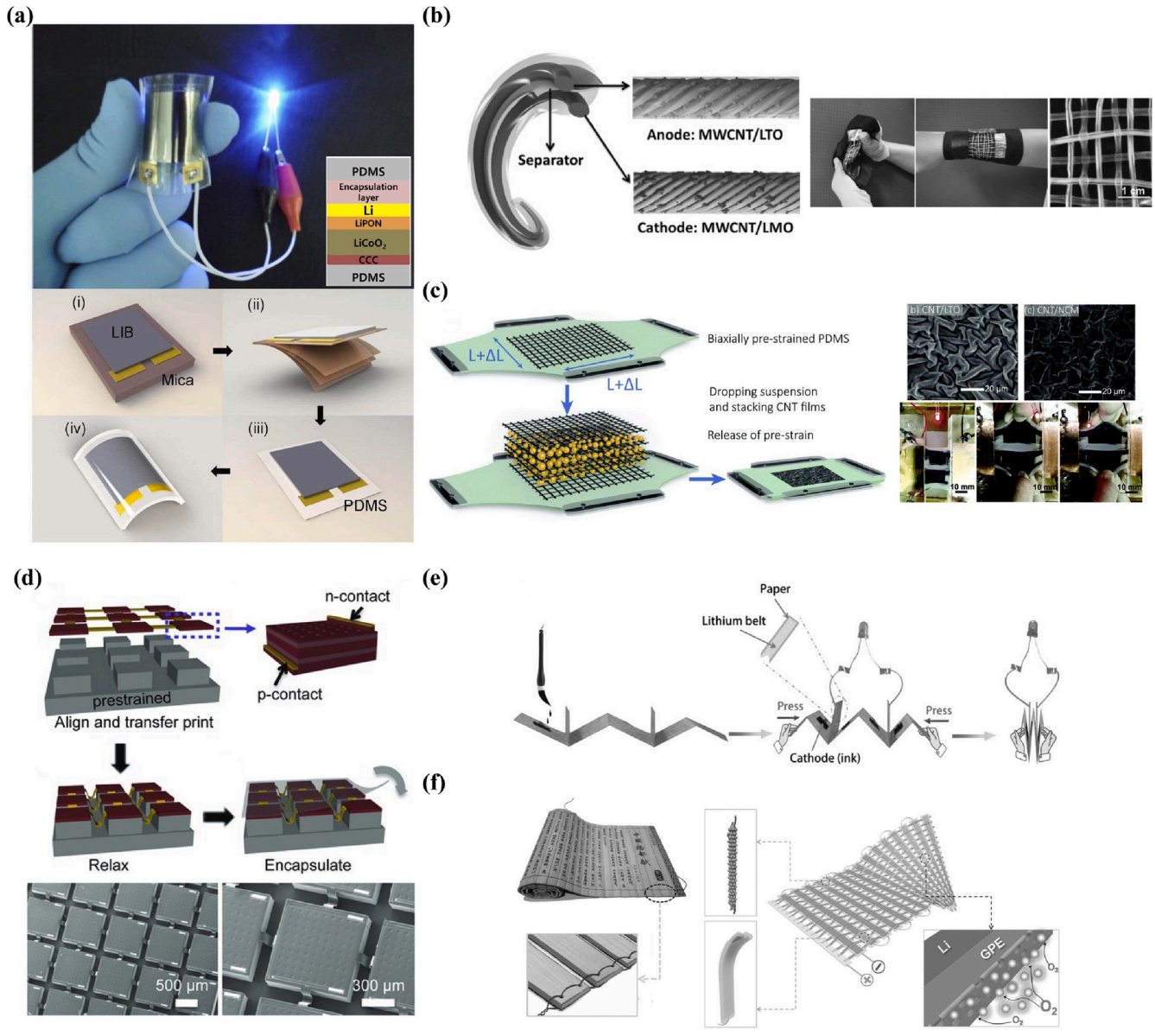

Fig. 7. (a) Thin film structure [100]. Reproduced with permission. Copyright 2012, American Chemical Society. (b) Fiber type structure [102]. Reproduced with permission. Copyright 2014, Wiley-VCH. (c) Wavy structure [105]. Reproduced with permission. Copyright 2018, The Royal Society of Chemistry. (d) Island connection structure [106]. Reproduced with permission. Copyright 2011, Wiley-VCH. (e) Paper folding structure [108]. Reproduced with permission. Copyright 2015, Wiley-VCH. (f) Bamboo slip structure [109]. Reproduced with permission. Copyright 2016, Wiley-VCH.

cells, and recently developed pouch cells and prismatic cells. The cylindrical cell contains a hard protective shell on the outside [99]. This kind of structure cannot withstand severe external deformation, so the design of new battery structure or assembly method is an important part to achieve FLIBs. The common FLIBs structures mainly include thin film, fiber type, wavy, island connection, paper folding, and bamboo slip structures, some of which are used in pouch cells and prismatic cells. The recent advances of these FLIB structures are reviewed in this section.

3.1. Thin film structure

Thin film structure is the most typical flexible battery structure. Layered battery components including electrodes and electrolytes are assembled by vertical stacking, and the external packaging materials of the batteries can be Al plastic films or flexible polymer substrates.

Lee et al. presented a thin-film FLIB using a universal transfer approach [100]. $LiCoO_2$ was used as the cathode, lithium phosphorus oxynitride was the electrolyte, lithium metal was the anode, and the outermost layer was the PDMS substrate (Fig. 7a). The battery had a strong bending capability, and can be integrated with a flexible light emitting diode (LED). By replacing the protective shell with a lighter, more flexible Al plastic film, pouch cells assembled with the thin film structure showed flexibility under bending. Passerini et al. prepared a flexible pouch cell, consisting of Ni-rich cathode, PEO-based ternary polymer electrolyte, and Li metal anode, which exhibited superior electrochemical performance [101].

The advantages of thin film structure are that the preparation process is simple and the mass production is convenient. How to further reduce the mass of the packaging material and the thickness of each component to improve the gravimetric and volumetric energy density is the focus of future researches.

3.2. Fiber type structure

Fiber type structure typically consists of either two twisted fiber electrodes or a coaxial cable configuration. Devices with the fiber type structure exhibits wearable feature for FLIBS through integration into cloths, wrist bands, necklace, gloves, masks or other similar goods in our daily life.

In a twisted structure, two fiber electrodes are intertwined together at a certain twisting angle to form a double-helix structure. Peng et al. developed a strategy to prepare fiber type FLIBs [102]. In this work, $Li_4Ti_5O_{12}$ and $LiMn_2O_4$ nanoparticles were scrolled into two aligned MWCNTs respectively (Fig. 7b), and the two composite yarns could be paired to obtain a fiber-type FLIB that could be further woven into lightweight, flexible, and stretchable battery textiles. Li et al. proposed a novel strategy to fabricate a stretchable lithium anode by infusing molten lithium into robust and flexible CNT fibers modified with lithiophilic ZnO nanowire arrays [103]. The lithium anode integrated a 3D structure of ZnO arrays with the admirable stretchability of CNT fibers. The symmetric cells based on these fibers demonstrated an excellent cyclic stability under a strain of 100%.

As for the typical coaxial structure, the flexible outer electrode is wound around the inner electrode with a separator between them, forming a core–shell architecture. Shin and Kim et al. produced a coaxial FLIB cable. A helical and hollow Ni–Sn-coated Cu wire was used as the anode and core in the coaxial structure. A separator was rolled outside the anode to separate the cathode from the anode, and the $LiCoO_2$ was then coated on a aluminum wire as the cathode and wound on the outside of the separator [104].

The fiber type structure is novel, and its weavability and stretchability greatly increase the application scenarios of FLIBs. However, this kind of structure may have problems such as protective layer breakage and electrolyte volatilization in practical use. In addition, low energy density is also an important factor limiting its application. Future research may focus on how to increase the length of the fiber electrodes, enhance the stability of the protective layer, and increase the energy density.

3.3. Wavy structure

By covering active materials on a pre-stretched elastic substrate and then removing the strain, a wavy structure can be formed on the surface of the active material film and substrate. When the applied strain is less than the pre-stretched strain, the wavy structure can be reversibly stretched and released while maintaining the integrity of the functional structure, thus obtaining high stretchability.

Wang et al. fabricated ultra-stretchable CNT composite electrodes by coating CNT films and active material powder on biaxially pre-strained PDMS substrates (Fig. 7c) [105]. The wrinkled structures that formed during the pre-straining and release process extended along the strain axis to protect the CNT composite structures from fracture. The CNT composites demonstrated excellent stability and high durability. The full FLIB consisting of stretchable CNT/LTO anode and CNT/NCM cathode was able to withstand 150% strain in different axes without large decreases in performance.

The method of pre-stretching can be used to transform materials that do not have stretchability but have great electrochemical activity, such as metal, carbon film, etc., into wavy structures that can withstand large strain. The preparation method is simple, and the stretchability of electrode can be easily controlled by the amount of pre-stretching. Therefore, it is a potential method for preparing stretchable FLIBs. The limitation of this method is that the maximum strain level the FLIBs can endure is determined by the upper stretching limit of the elastic substrate. In addition, excessive pre-stretching may cause the electrode surface to form a serious fold after removing the pre-stretching, which lead to the detachment of active materials and the increase of interface contact resistance.

3.4. Island connection structure

In 2011, Rogers et al. proposed a new flexible structure and firstly applied to the stretchable solar modules that use ultrathin, single junction GaAs solar cells [106]. As shown in Fig. 7d, elastomeric substrates with surface relief in geometries was used that confined strains at the locations of the interconnections and away from the devices. Because this structure consisted of island-shape units and stretchable wires, it is named island connection structure here.

Rogers et al. extended the island connection structure to FLIBs in 2013 [107]. In this structure, small, traditional LIBs without flexibility were arranged in a flat island form, and were connected with bent stretchable wires. Under applied strain, the bent wires between the structural units were stretched to absorb the strain, thereby ensuring the structural integrity of the functional units and allowing the entire device to withstand mechanical deformation. The advantages of this structure are that the basic structural units are traditional LIBs, their electrochemical performances are relatively stable, and the preparation process is very mature. The structure of such a planar network allows the device to withstand strain in different directions. For such a structure in which the in-plane curved wire is connected, the tensile strength can be improved only by increasing the length of the curved wire or reducing the area of the island-shaped functional unit in a limited space. This can result in a reduction in the area utilization, which affects the energy density of the entire stretchable battery device.

3.5. Other structures

Some other structures have emerged in the study of flexible batteries, including FLIBs and flexible lithium-air batteries (FLABs). As shown in Fig. 7e and f, Zhang et al. introduced ancient Chinese calligraphy art in the research of FLABs, and proposed paper folding and bamboo slip structures [108,109]. The new designs of these flexible battery

structures can be applied in different material systems and provide a novel route to convert traditional LIBs to FLIBs. Some special structures can make the traditional LIBs that do not have flexibility gain the ability to resist deformation. The design of more ideal flexible battery structures makes the mass and volume occupied by non-active substances in the structure smaller, so as to obtain FLBs with higher gravimetric and volumetric energy densities.

4. Conclusion

In summary, with the development of flexible electronic products, the great prospects for FLIBs are unquestionable, and the progress of FLIBs will certainly promote further advances of flexible electronic products. In this review, two effective ways to assemble FLIBs are summarized: the fabrication of flexible battery components and the design of flexible battery structures. In the aspect of the fabrication of flexible battery components, flexible electrodes and flexible electrolytes are the two most critical elements. The design of flexible electrodes usually starts with current collectors and binders. Carbon, polymer, MXene, and other flexible materials are commonly used to replace the current collectors or binders in traditional LIBs, thus achieving the purpose of flexibility. In addition, flexible polymers or layered materials that can be used as active materials for LIBs are an ideal choice for FLIBs. As for flexible electrolytes, flexible polymer is an effective alternative to the liquid electrolyte of traditional LIBs, but the low ionic conductivity and narrow electrochemical window of polymer electrolytes set limitation for use in FLIBs. Inorganic-organic composite polymer solid electrolyte and gel electrolyte are two promising electrolytes, which can effectively improve the ionic conductivity and electrochemical stability. In addition, the design of flexible battery structures can make the original rigid LIBs to obtain a certain degree of flexibility, such as thin film, fiber type, wavy, island connection, paper folding, and bamboo slip structures. These studies have improved the performance of FLIBs and brought them closer to practical application, but challenges of FLIBs have also been exposed.

At present, there exist the following main factors that hinder the applications of FLIBs: the gravimetric and volumetric energy densities of the FLIBs are still not high enough; the capacity retention and cycle life of FLIBs are limited after cyclic mechanical deformations; high rate and high-temperature/low-temperature performances of FLIBs are still rarely studied; there are still difficulties in automated production processes, and the cost of battery preparation is high. The development of FLIBs in the future may focus on the following aspects:

(i) Preparation of flexible electrode materials with better performance. FLIBs need to withstand large deformations, so the requirements for electrode materials are high. Carbon materials have become a research hot spot of flexible electrodes due to its high conductivity, excellent mechanical properties, and high stability. Flexible carbon materials have excellent conductivity and flexibility, which can be combined with active materials to play an important role in FLIBs. At present, the problems that need to be solved by flexible electrodes are electrode structure design for high-load active materials, active materials with higher energy density, and safety problem of flexible electrodes.

(ii) Development of flexible polymer-based electrolytes. Polymer-based solid or gel electrolyte lithium can solve the leakage problem of the current organic liquid electrolyte in FLIBs. However, due to the special lithium ion transport mechanism, these electrolytes generally have low ionic conductivity, unsatisfactory rate performance, narrow electrochemical window, low active material loading, and complicated preparation process, limiting the large-scale industrialization of FLIBs. Therefore, further optimization of the preparation process of polymer electrolytes, development of high-performance flexible electrolytes, and selection of suitable electrolytes for different flexible battery systems are the keys in future research.

(iii) Design of battery structure. New structures such as fibrous electrodes, interpenetrating island structures, and pre-tensioned structures are shown. It is also an effective solution to achieve flexibility through structural design methods. Moreover, the design of this structure can achieve the integration of FLIBs, which greatly expands the application scenarios. At the same time, it is necessary to develop more flexible structures and to optimize the structure of the FLIBs, including the interface between the electrode, the electrolyte, and the substrate.

(iv) Improvement and breakthrough of the electrochemical system. The current reaction system of FLIBs is derived from LIBs with lithium-ion insertion/extraction, but the energy density of this system is relatively low. In the future, an electrochemical system with a higher theoretical energy density such as a flexible lithium metal battery system or a flexible lithium-air battery is an effective strategy. Some researchers have already performed pioneer work in this area [110,111].

(v) Optimization of packaging material. The packaging material makes the FLIBs have better resistance to external environmental influences and structural stability and is an essential component for protecting the battery in the FLIBs. However, the introduction of packaging materials will lead to the loss of the overall gravimetric and volumetric energy density of the battery. Therefore, the development of a thinner, more flexible and stable packaging material is also demanding to obtain high performance FLIBs.

(vi) Exploration of automated production processes. It is necessary to explore a large-scale automated approach to the production of FLIBs while ensuring lower costs, mainly including the mass production of flexible electrolytes and flexible electrodes, assembly of flexible batteries, integration of flexible batteries, etc. Based on the current mature LIB production process, new material preparation technologies, such as 3D printing and film preparation technology should be developed.

(vii) Developing more application scenarios. The development of special FLIBs with more functional features besides flexibility, such as biocompatible properties, extreme temperature characteristics, etc., can be used for a wider range of applications, and meet the needs of a variety of electronic devices. In this respect, there is certainly a broader demand for the practical application market, but this type of battery adds more functions than simple flexibility, and certainly there are more problems need to be solved.

CRediT authorship contribution statement

Zhenhan Fang: Conceptualization, Investigation, Writing - original draft. **Jing Wang:** Conceptualization, Investigation, Writing - original draft. **Hengcai Wu:** Writing - original draft. **Qunqing Li:** Conceptualization, Supervision. **Shoushan Fan:** Conceptualization, Supervision. **Jiaping Wang:** Conceptualization, Supervision, Writing - review & editing.

Acknowledgements

This work was supported by the National Basic Research Program of China (2019YFA0705700) and the National Natural Science Foundation of China (Grant Nos. 51872158 and 51532008).

References

[1] Arokia Nathan, et al., Flexible electronics: the next ubiquitous platform, Proc. IEEE 100 (2012) 1486–1517, https://doi.org/10.1109/JPROC.2012.2190168.
[2] Claire M. Lochner, et al., All-organic optoelectronic sensor for pulse oximetry, Nat. Commun. 5 (2014) 5745, https://doi.org/10.1038/ncomms6745.

[3] Veena Misra, et al., Flexible technologies for self-powered wearable health and environmental sensing, Proc. IEEE 103 (4) (2015) 665–681, https://doi.org/10.1109/JPROC.2015.2412493.

[4] Wenzhao Jia, et al., Wearable textile biofuel cells for powering electronics, J. Mater. Chem. A 2 (43) (2014) 18184–18189, https://doi.org/10.1039/C4TA04796F.

[5] Zeming Song, et al., Kirigami-based stretchable lithium-ion batteries, Sci. Rep. 5 (2015) 10988, https://doi.org/10.1038/srep10988.

[6] Matteo Stoppa, et al., Wearable electronics and smart textiles: a critical review, Sensors 14 (7) (2014) 11957–11992, https://doi.org/10.3390/s140711957.

[7] Aminy E. Ostfeld, et al., High-performance flexible energy storage and harvesting system for wearable electronics, Sci. Rep. 6 (2016) 26122, https://doi.org/10.1038/srep26122.

[8] K. Mizushima, et al., LixCoO2 (0< x<-1): a new cathode material for batteries of high energy density, Mater. Res. Bull. 15 (6) (1980) 783–789, https://doi.org/10.1016/0025-5408(80)90012-4.

[9] Bruce Dunn, et al., Electrical energy storage for the grid: a battery of choices, Science 334 (6058) (2011) 928–935, https://doi.org/10.1126/science.1212741.

[10] J.M. Tarascon, et al., Issues and challenges facing rechargeable lithium batteries, Nature 414 (6861) (2001), https://doi.org/10.1038/35104644, 359-67.

[11] Yongmin He, et al., An overview of carbon materials for flexible electrochemical capacitors, Nanoscale 5 (19) (2013) 8799, https://doi.org/10.1039/C3NR02157B.

[12] Guangmin Zhou, et al., Progress in flexible lithium batteries and future prospects, Energy Environ. Sci. 7 (4) (2014) 1307–1338, https://doi.org/10.1039/c3ee43182g.

[13] Lei Wen, et al., Carbon nanotubes and graphene for flexible electrochemical energy storage: from materials to devices, Adv. Mater. 28 (22) (2016) 4306–4337, https://doi.org/10.1002/adma.201504225.

[14] Ke Wang, et al., Super-aligned carbon nanotube films as current collectors for lightweight and flexible lithium ion batteries, Adv. Funct. Mater. 23 (7) (2013) 846–853, https://doi.org/10.1002/adfm.201202412.

[15] Ting Liu, et al., Engineering the surface/interface of horizontally oriented carbon nanotube macrofilm for foldable lithium-ion battery withstanding variable weather, Adv. Energy Mater 8 (30) (2018) 1802349, https://doi.org/10.1002/aenm.201802349.

[16] Shu Luo, et al., Binder-free LiCoO2/carbon nanotube cathodes for high-performance lithium ion batteries, Adv. Mater. 24 (17) (2012) 2294–2298, https://doi.org/10.1002/adma.201104720.

[17] Kunlei Zhu, et al., Free-standing, binder-free titania/super-aligned carbon nanotube Anodes for flexible and fast-charging Li-ion batteries, ACS Sustain. Chem. Eng. 6 (3) (2018) 3426–3433, https://doi.org/10.1021/acssuschemeng.7b03671.

[18] Zainab Karam, et al., Development of surface-engineered tape-casting method for fabricating freestanding carbon nanotube sheets containing Fe2O3 nanoparticles for flexible batteries, Adv. Eng. Mater. 20 (6) (2018) 1701019, https://doi.org/10.1002/adem.201701019.

[19] Lei Shen, et al., Versatile MnO2/CNT putty-like composites for high-rate lithium-ion batteries, Adv. Mater. Interfaces 5 (14) (2018), https://doi.org/10.1002/admi.201800362, 1800362.

[20] Andre Konstantin Geim, Graphene: status and prospects, *Science* 324 (5934) (2009) 1530–1534, https://doi.org/10.1126/science.1158877.

[21] Geng Zhong, et al., Ultralong MnO@ C nanowires with internal voids anchored between graphene as a robust high performance anode for flexible Li-Ion battery, Electrochim. Acta 296 (2019) 276–282, https://doi.org/10.1016/j.electacta.2018.09.199.

[22] Hao Wen, et al., Two-phase interface hydrothermal synthesis of binder-free SnS 2/graphene flexible paper electrodes for high-performance Li-ion batteries, RSC Adv. 9 (41) (2019) 23607–23613, https://doi.org/10.1039/C9RA03397A.

[23] Zongping Chen, et al., Three-dimensional flexible and conductive interconnected graphene networks grown by chemical vapour deposition, Nat. Mater. 10 (6) (2011) 424, https://doi.org/10.1038/nmat3001.

[24] Na Li, et al., Flexible graphene-based lithium ion batteries with ultrafast charge and discharge rates, Proc. Natl. Acad. Sci. Unit. States Am. 109 (43) (2012) 17360–17365, https://doi.org/10.1073/pnas.1210072109.

[25] Tiancai Jiang, et al., Porous Fe2O3 nanoframeworks encapsulated within three-dimensional graphene as high-performance flexible anode for lithium-ion battery, ACS Nano 11 (5) (2017) 5140–5147, https://doi.org/10.1021/acsnano.7b02198.

[26] Runwei Mo, et al., 3D nitrogen-doped graphene foam with encapsulated germanium/nitrogen-doped graphene yolk-shell nanoarchitecture for high-performance flexible Li-ion battery, Nat. Commun. 8 (2017) 13949, https://doi.org/10.1038/ncomms13949.

[27] Darrell H. Reneker, et al., Electrospinning jets and polymer nanofibers, Polymer 49 (10) (2008) 2387–2425, https://doi.org/10.1016/j.polymer.2008.02.002.

[28] Ya-Li Li, et al., Direct spinning of carbon nanotube fibers from chemical vapor deposition synthesis, Science 304 (5668) (2004) 276–278, https://doi.org/10.1126/science.1094982.

[29] Yudi Kuang, et al., Conductive cellulose nanofiber enabled thick electrode for compact and flexible energy storage devices, Adv. Energy Mater 8 (33) (2018), https://doi.org/10.1002/aenm.201802398, 1802398.

[30] Xueyan Huang, et al., Hierarchical Fe2O3@ CNF fabric decorated with MoS2 nanosheets as a robust anode for flexible lithium-ion batteries exhibiting ultrahigh areal capacity, J. Mater. Chem. A 6 (35) (2018) 16890–16899, https://doi.org/10.1039/C8TA04341H.

[31] Wenjie Zhang, et al., Steam selective etching: a strategy to effectively enhance the flexibility and suppress the volume change of carbonized paper-supported electrodes, ACS Nano 13 (5) (2019) 5731–5741, https://doi.org/10.1021/acsnano.9b01173.

[32] Mingyue Wang, et al., Binder-free flower-like SnS2 nanoplates decorated on the graphene as a flexible anode for high-performance lithium-ion batteries, J. Alloys Compd. 774 (2019) 601–609, https://doi.org/10.1016/j.jallcom.2018.09.378.

[33] Tianyue Zheng, et al., Molecular spring enabled high-performance anode for lithium ion batteries, Polymers 9 (12) (2017) 657, https://doi.org/10.3390/polym9120657.

[34] Kamran Amin, et al., A carbonyl compound-based flexible cathode with superior rate performance and cyclic stability for flexible lithium-ion batteries, Adv. Mater. 30 (4) (2018) 1703868, https://doi.org/10.1002/adma.201703868.

[35] Lie Ma, et al., Solution-processed organic PDI/CB/TPU cathodes for flexible lithium ion batteries, Electrochim *Acta*319 (2019) 201–209, https://doi.org/10.1016/j.electacta.2019.06.153.

[36] Michael Ghidiu, et al., Conductive two-dimensional titanium carbide 'clay' with high volumetric capacitance, Nature 516 (7529) (2014) 78, https://doi.org/10.1038/nature13970.

[37] Chuanliang Wei, et al., Room-temperature liquid metal confined in MXene paper as a flexible, freestanding, and binder-free anode for next-generation lithium-ion batteries, Small 15 (2019) 46, https://doi.org/10.1002/smll.201903214.

[38] Qian Zhao, et al., Flexible 3D porous MXene foam for high-performance lithium-ion batteries, Small 15 (51) (2019), https://doi.org/10.1002/smll.201904293.

[39] Peng Zhang, et al., A flexible Si@ C electrode with excellent stability employing an MXene as a multifunctional binder for lithium-ion batteries, ChemSusChem (2019), https://doi.org/10.1002/cssc.201901497.

[40] Jinli Wu, et al., Molecularly coupled two-dimensional titanium oxide and carbide sheets for wearable and high-rate quasi-solid-state rechargeable batteries, Adv. Funct. Mater. 29 (30) (2019), https://doi.org/10.1002/adfm.201901576, 1901576.

[41] Yannick Philipp, Stenzel, et al., Chromatographic techniques in the research area of lithium ion batteries: current state-of-the-art, Separations 6 (2) (2019) 26, https://doi.org/10.3390/separations6020026" \o "10.3390/separations6020026"10.3390/separations6020026. HYPERLINK.

[42] Venkataraman Thangadurai, et al., Novel fast lithium ion conduction in garnet-type Li5La3M2O12 (M= Nb, Ta), J. Am. Ceram. Soc. 86 (3) (2003) 437–440, https://doi.org/10.1111/j.1151-2916.2003.tb03318.x.

[43] Ramaswamy Murugan, et al., Fast lithium ion conduction in garnet-type Li7La3Zr2O12, Angew. Chem. Int. Ed. 46 (41) (2007) 7778–7781, https://doi.org/10.1002/anie.200701144.

[44] Noriaki Kamaya, et al., A lithium superionic conductor, Nat. Mater. 10 (9) (2011) 682, https://doi.org/10.1038/NMAT3066.

[45] Fuminori Mizuno, et al., New, highly ion-conductive crystals precipitated from Li2S–P2S5 glasses, Adv. Mater. 17 (7) (2005) 918–921, https://doi.org/10.1002/adma.200401286.

[46] Yongyao Xia, et al., Thermal and electrochemical stability of cathode materials in solid polymer electrolyte, J. Power Sources 92 (1–2) (2001) 234–243, https://doi.org/10.1016/S0378-7753(00)00533-4.

[47] Weidong Zhou, et al., Double-layer polymer electrolyte for high-voltage all-solid-state rechargeable batteries, Adv. Mater. 31 (4) (2019), https://doi.org/10.1002/adma.201805574, 1805574.

[48] Jiayu Wan, et al., Ultrathin, flexible, solid polymer composite electrolyte enabled with aligned nanoporous host for lithium batteries, Nat. Nanotechnol. (2019) 1, https://doi.org/10.1038/s41565-019-0465-3.

[49] Zi-Jian He, et al., Poly (ethylene carbonate)-based electrolytes with high concentration Li salt for all-solid-state lithium batteries, Rare Met. 37 (6) (2018) 488–496, https://doi.org/10.1007/s12598-018-1017-y.

[50] Bing Sun, et al., Polycarbonate-based solid polymer electrolytes for Li-ion batteries, Solid State Ionics 262 (2014) 738–742, https://doi.org/10.1016/j.ssi.2013.08.014.

[51] Yang Li, et al., Ambient temperature solid-state Li-battery based on high-salt-concentrated solid polymeric electrolyte, J. Power Sources 397 (2018) 95–101, https://doi.org/10.1016/j.jpowsour.2018.05.050.

[52] Elmér, Anette Munch, et al., Synthesis and characterization of poly (ethylene oxide-co-ethylene carbonate) macromonomers and their use in the preparation of crosslinked polymer electrolytes, J. Polym. Sci., Part A: Polym. Chem. 44 (7) (2006) 2195–2205, https://doi.org/10.1002/pola.21324.

[53] Jonas Mindemark, et al., Copolymers of trimethylene carbonate and ε-caprolactone as electrolytes for lithium-ion batteries, Polymer 63 (2015) 91–98, https://doi.org/10.1016/j.polymer.2015.02.052.

[54] Yiqun Yang, et al., Poly (propylene carbonate) interpenetrating cross-linked poly (ethylene glycol) based polymer electrolyte for solid-state lithium batteries, ECS Trans 85 (13) (2018) 53–59, https://doi.org/10.1149/08513.0053ecst.

[55] Renjie Chen, et al., An investigation of functionalized electrolyte using succinonitrile additive for high voltage lithium-ion batteries, J. Power Sources 306 (2016) 70–77, https://doi.org/10.1016/j.jpowsour.2015.10.105.

[56] Pierre-Jean Alarco, et al., The plastic-crystalline phase of succinonitrile as a universal matrix for solid-state ionic conductors, Nat. Mater. 3 (7) (2004) 476, https://doi.org/10.1038/nmat1158.

[57] Appetecchi, Giovanni Battista, et al., High-performance gel-type lithium electrolyte membranes, Electrochem. Commun. 1 (2) (1999) 83–86, https://doi.org/10.1016/S1388-2481(99)00011-9.

[58] Yin Zheng Liang, et al., Preparation and characterization of electrospun PVDF/PMMA composite fibrous membranes-based separator for lithium-ion batteries, Adv. Mater. Res. 750 (2013) 1914–1918. https://doi.org/10.4028/www.scientific.net/AMR.750-752.1914.

[59] David G. Mackanic, et al., Crosslinked poly (tetrahydrofuran) as a loosely coordinating polymer electrolyte, Adv. Energy Mater 8 (25) (2018), https://doi.org/10.1002/aenm.201800703, 1800703.
[60] Gen Zhang, et al., Accumulation of glassy poly (ethylene oxide) anchored in a covalent organic framework as a solid-state Li+ electrolyte, J. Am. Chem. Soc. 141 (3) (2018) 1227–1234, https://doi.org/10.1021/jacs.8b07670.
[61] Peter V. Wright, Polymer electrolytes—the early days, Electrochim. Acta 43 (10–11) (1998) 1137–1143, https://doi.org/10.1016/S0013-4686(97)10011-1.
[62] Takefumi Okumura, et al., Lithium ion conductive properties of aliphatic polycarbonate, Solid State Ionics 267 (2014) 68–73, https://doi.org/10.1016/j.ssi.2014.09.011.
[63] Jonas Mindemark, et al., High-performance solid polymer electrolytes for lithium batteries operational at ambient temperature, J. Power Sources 298 (2015) 166–170, https://doi.org/10.1016/j.jpowsour.2015.08.035.
[64] Bing Sun, et al., Polycarbonate-based solid polymer electrolytes for Li-ion batteries, Solid State Ionics 262 (2014) 738–742, https://doi.org/10.1016/j.ssi.2013.08.014.
[65] Jianjun Zhang, et al., Safety-reinforced poly (propylene carbonate)-based All-solid-state polymer electrolyte for ambient-temperature solid polymer lithium batteries, Adv. Energy Mater 5 (24) (2015) 1501082, https://doi.org/10.1002/aenm.201501082.
[66] C.R. Yang, et al., Conductive behaviour of lithium ions in polyacrylonitrile, J. Power Sources 62 (1) (1996) 89–93, https://doi.org/10.1016/S0378-7753(96)02414-7.
[67] Chaole Li, et al., Preparation and characterization of PAN-LATP composite solid-state electrolyte, Scientia Sinica Chimica 48 (8) (2018) 964–971, https://doi.org/10.1360/N032018-00062.
[68] Y.J. Shen, et al., Porous PVDF with LiClO4 complex as 'solid' and 'wet' polymer electrolyte, Solid State Ionics 175 (1–4) (2004) 747–750, https://doi.org/10.1016/j.ssi.2003.10.020.
[69] F. Croce, et al., Nanocomposite polymer electrolytes for lithium batteries, Nature 394 (6692) (1998) 456, https://doi.org/10.1557/PROC-496-511.
[70] Xiaokun Zhang, et al., Vertically aligned and continuous nanoscale ceramic–polymer interfaces in composite solid polymer electrolytes for enhanced ionic conductivity, Nano Lett. 18 (6) (2018) 3829–3838, https://doi.org/10.1021/acs.nanolett.8b01111.
[71] Jiwoong Bae, et al., Designing 3D nanostructured garnet frameworks for enhancing ionic conductivity and flexibility in composite polymer electrolytes for lithium batteries, Energy Storage Mater 15 (2018) 46–52, https://doi.org/10.1016/j.ensm.2018.03.016.
[72] Xue Zhang, et al., Synergistic coupling between Li6. 75La3Zr1. 75Ta0. 25O12 and poly (vinylidene fluoride) induces high ionic conductivity, mechanical strength, and thermal stability of solid composite electrolytes, J. Am. Chem. Soc. 139 (39) (2017) 13779–13785, https://doi.org/10.1021/jacs.7b06364.
[73] Hua Xie, et al., Flexible garnet solid-state electrolyte membranes enabled by tile-and-grout design, ACS Energy Lett 4 (11) (2019) 2668–2674, https://doi.org/10.1021/acsenergylett.9b01847.
[74] Weidong Zhou, et al., Polymer lithium-garnet interphase for an all-solid-state rechargeable battery, Nano energy 53 (2018) 926–931, https://doi.org/10.1016/j.nanoen.2018.09.004.
[75] Brian M. Wiers, et al., A solid lithium electrolyte via addition of lithium isopropoxide to a metal–organic framework with open metal sites, J. Am. Chem. Soc. 133 (37) (2011) 14522–14525, https://doi.org/10.1021/ja205827z.
[76] Jian-Fang Wu, et al., MOF-derived nanoporous multifunctional fillers enhancing the performances of polymer electrolytes for solid-state lithium batteries, J. Mater. Chem. A 7 (6) (2019) 2653–2659, https://doi.org/10.1039/c8ta10124h.
[77] Hanyu Huo, et al., Anion-immobilized polymer electrolyte achieved by cationic metal-organic framework filler for dendrite-free solid-state batteries, Energy Storage Mater 18 (2019) 59–67, https://doi.org/10.1016/j.ensm.2019.01.007.
[78] G. Feuillade, et al., Ion-conductive macromolecular gels and membranes for solid lithium cells, J. Appl. Electrochem. 5 (1) (1975) 63–69, https://doi.org/10.1007/bf00625960.
[79] G. Nagasubramanian, et al., 12-Crown-4 Ether-assisted enhancement of ionic conductivity and interfacial kinetics in polyethylene oxide electrolytes, J. Electrochem. Soc. 137 (12) (1990) 3830–3835, https://doi.org/10.1149/1.2086309.
[80] G.B. Appetecchi, et al., A lithium ion polymer battery, Electrochim. Acta 43 (9) (1998) 1105–1107, https://doi.org/10.1016/S0013-4686(97)10117-7.
[81] J.Y. Song, et al., Review of gel-type polymer electrolytes for lithium-ion batteries, J. Power Sources 77 (2) (1999) 183–197, https://doi.org/10.1016/S0378-7753(98)00193-1.
[82] F. Croce, et al., Interfacial phenomena in polymer-electrolyte cells: lithium passivation and cycleability, J. Power Sources 43 (1–3) (1993) 9–19, https://doi.org/10.1016/0378-7753(93)80097-9.
[83] Huang Hong, et al., Studies on PAN-based lithium salt complex, Electrochim. Acta 37 (9) (1992) 1671–1673, https://doi.org/10.1016/0013-4686(92)80135-9.
[84] Zhaoxiang Wang, et al., Investigation of the position of Li+ ions in a polyacrylonitrile-based electrolyte by Raman and infrared spectroscopy, Electrochim. Acta 41 (9) (1996) 1443–1446, https://doi.org/10.1016/0013-4686(95)00392-4.
[85] H.S. Choe, et al., Preparation and characterization of poly (vinyl sulfone)-and poly (vinylidene fluoride)-based electrolytes, Electrochim. Acta 40 (13–14) (1995) 2289–2293, https://doi.org/10.1016/0013-4686(95)00180-M.
[86] Zhong Ren, et al., A microporous gel electrolyte based on poly (vinylidene fluoride-co-hexafluoropropylene)/fully cyanoethylated cellulose derivative blend for lithium-ion battery, Electrochim. Acta 54 (6) (2009) 1888–1892, https://doi.org/10.1016/j.electacta.2008.10.011.
[87] Madhuryya Deka, et al., Enhanced electrical and electrochemical properties of PMMA–clay nanocomposite gel polymer electrolytes, Electrochim. Acta 55 (5) (2010) 1836–1842, https://doi.org/10.1016/j.electacta.2009.10.076.
[88] Stephan A Manuel, et al., Poly (vinylidene fluoride-hexafluoropropylene)(PVdF-HFP) based composite electrolytes for lithium batteries, Eur. Polym. J. 42 (8) (2006) 1728–1734, https://doi.org/10.1016/j.eurpolymj.2006.02.006.
[89] S. Ferrari, et al., Lithium ion conducting PVdF-HFP composite gel electrolytes based on N-methoxyethyl-N-methylpyrrolidinium bis (trifluoromethanesulfonyl)-imide ionic liquid, J. Power Sources 195 (2) (2010) 559–566, https://doi.org/10.1016/j.jpowsour.2009.08.015.
[90] Youhao Liao, et al., Cycling performance improvement of polypropylene supported poly (vinylidene fluoride-co-hexafluoropropylene)/maleic anhydride-grated-polyvinylidene fluoride based gel electrolyte by incorporating nano-Al2O3 for full batteries, J. Membr. Sci. 507 (2016) 126–134, https://doi.org/10.1016/j.memsci.2016.02.001.
[91] Guanghai Chen, et al., A flexible dual-ion battery based on PVDF-HFP-modified gel polymer electrolyte with excellent cycling performance and superior rate capability, Adv. Energy Mater 8 (25) (2018), https://doi.org/10.1002/aenm.201801219, 1801219.
[92] J. Fuller, et al., Ionic liquid-polymer gel electrolytes, J. Electrochem. *Soc*144 (4) (1997) L67–L70, https://doi.org/10.1149/1.1837555.
[93] HoSeok Park, et al., Interionic interactions of binary gels consisting of pyrrolidinium-based zwitterionic compounds and lithium salts, J. Phys. Chem. B 115 (8) (2011) 1743–1750, https://doi.org/10.1021/jp1062176.
[94] Xinpei Gao, et al., Temperature-responsive proton-conductive liquid crystals formed by the self-assembly of zwitterionic ionic liquids, RSC Adv. 5 (78) (2015) 63732–63737, https://doi.org/10.1039/C5RA10830F.
[95] Le Yu, et al., Highly tough, Li-metal compatible organic–inorganic double-network solvate ionogel, Adv. Energy Mater 9 (22) (2019), https://doi.org/10.1002/aenm.201900257, 1900257.
[96] Xi Chen, et al., Fully integrated design of a stretchable solid-state lithium-ion full battery, Adv. Mater. 31 (43) (2019), https://doi.org/10.1002/adma.201904648.
[97] Feng-Quan Liu, et al., Upgrading traditional liquid electrolyte via in situ gelation for future lithium metal batteries, Sci. Adv 4 (10) (2018), https://doi.org/10.1126/sciadv.aat5383 eaat5383.
[98] Haiyang Liao, et al., Dendrite-free lithium deposition induced by mechanical strong sponge-supported unique 3D cross-linking polymer electrolyte for lithium metal batteries, J. Power Sources 435 (2019) 226748, https://doi.org/10.1016/j.jpowsour.2019.226748.
[99] Peidong Yang, et al., Towards systems materials engineering, Nat. Mater. 11 (7) (2012) 560, https://doi.org/10.1038/nmat3367.
[100] Min Koo, et al., Bendable inorganic thin-film battery for fully flexible electronic systems, Nano Lett. 12 (9) (2012) 4810–4816, https://doi.org/10.1021/nl302254v.
[101] Zhen Chen, et al., 4-V flexible all-solid-state lithium polymer batteries, Nanomater. Energy 64 (2019) 103986, https://doi.org/10.1016/j.nanoen.2019.103986.
[102] Jing Ren, et al., Elastic and wearable wire-shaped lithium-ion battery with high electrochemical performance, Angew. Chem. Int. Ed. 53 (30) (2014) 7864–7869, https://doi.org/10.1002/anie.201402388.
[103] Xianshu Wang, et al., Stretchable fiber-shaped lithium metal anode, Energy Storage Mater 22 (2019) 179–184, https://doi.org/10.1016/j.ensm.2019.01.013.
[104] Yo Han Kwon, et al., Cable-type flexible lithium ion battery based on hollow multi-helix electrodes, Adv. Mater. 24 (38) (2012) 5192–5197, https://doi.org/10.1002/adma.201202196.
[105] Yang Yu, et al., Ultrastretchable carbon nanotube composite electrodes for flexible lithium-ion batteries, Nanoscale 10 (42) (2018) 19972–19978, https://doi.org/10.1039/C8NR05241G.
[106] Jongho Lee, et al., Stretchable GaAs photovoltaics with designs that enable high areal coverage, Adv. Mater. 23 (8) (2011) 986–991, https://doi.org/10.1002/adma.201003961.
[107] Sheng Xu, et al., Stretchable batteries with self-similar serpentine interconnects and integrated wireless recharging systems, Nat. Commun. 4 (2013) 1543, https://doi.org/10.1038/ncomms2553.
[108] Qing-Chao Liu, et al., Flexible and foldable Li–O2 battery based on paper-ink cathode, Adv. Mater. 27 (48) (2015) 8095–8101, https://doi.org/10.1002/adma.201503025.
[109] Qing-Chao Liu, et al., A flexible and wearable lithium–oxygen battery with record energy density achieved by the interlaced architecture inspired by bamboo slips, Adv. Mater. 28 (38) (2016) 8413–8418, https://doi.org/10.1002/adma.201602800.
[110] Jian Chang, et al., Flexible and stable high-energy lithium-sulfur full batteries with only 100% oversized lithium, Nat. Commun. 9 (1) (2018) 1–11, https://doi.org/10.1038/s41467-018-06879-7.
[111] Jung-Hwan Kim, et al., Nanomat Li–S batteries based on all-fibrous cathode/separator assemblies and reinforced Li metal anodes: towards ultrahigh energy density and flexibility, Energy Environ. Sci. 12 (1) (2019) 177–186, https://doi.org/10.1039/C8EE01879K.